



Technische Universität Darmstadt
Fachgebiet Strömungslehre und Aerodynamik
Leiter: Prof. Dr.-Ing. habil. C. Tropea



Flow computations and experiments in interaction

at Chair of Fluid Mechanics and Aerodynamics, TU Darmstadt

S. Jakirlić and C. Tropea

s.jakirlic@sla.tu-darmstadt.de

*Computational illustration by
R. Jester-Zürker, S. Grundmann, H.-D. Wilhelm and S. Jakirlic*

Technologietag ERCOFTAC Süddeutschland, Stuttgart, 30. September, 2005

Computational activities at FG SLA

■ Computational methods

➤ RANS, LES, hybrid RANS/LES (DES),

■ Advanced Turbulence Models (development)

➤ Near-Wall Second-Moment Closures

➤ Homogeneous dissipation concept

➤ Hybrid RANS (EVM/RSM) modelling strategy

➤ Hybrid RANS/LES: zonal and seamless approaches

■ LES/DES Simulations

➤ Turbulent flow separation control: periodically perturbed backward-facing step flow, flow over a 2-D hump; swirling/rotating flows,...

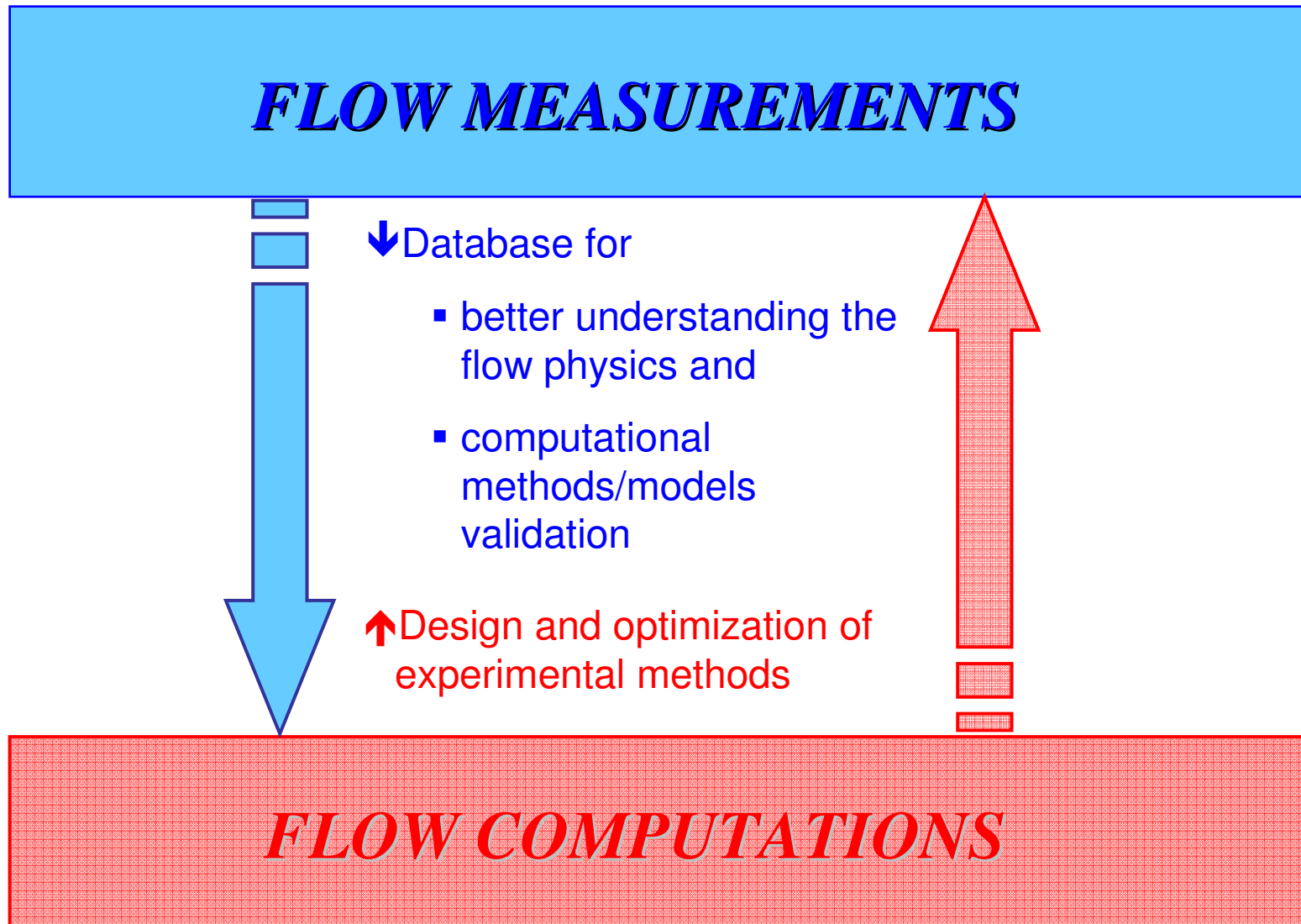
■ Flow geometries: flow past an aircraft configuration (airfoils, wings), swirl combustors,..., confined (wall bounded) flows, flows over bluff bodies,...

■ Mean flow and turbulence phenomena: PG-effects, (unsteady) separating and reattaching flows, swirling and rotating flows, flows with mean compression,..., flows with variable properties (density, viscosity); convective heat transfer,...

■ Two-phase flows: (Euler/Euler and Euler/Lagrange schemes) evaporation, wall impact; (VOF) single droplet and spray impact,...

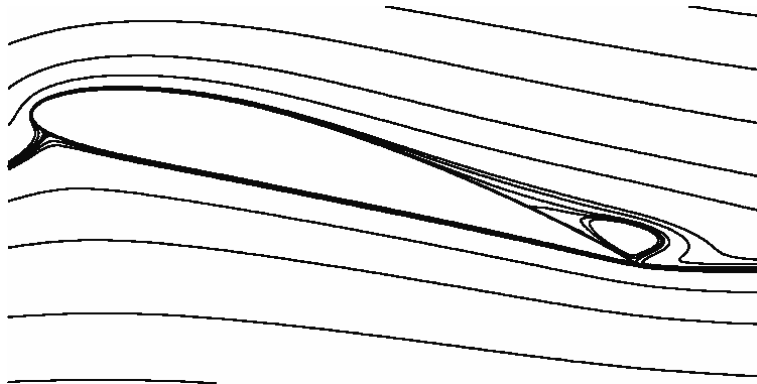
■ **Strong interaction between experimental and computational work**

Introduction/Motivation

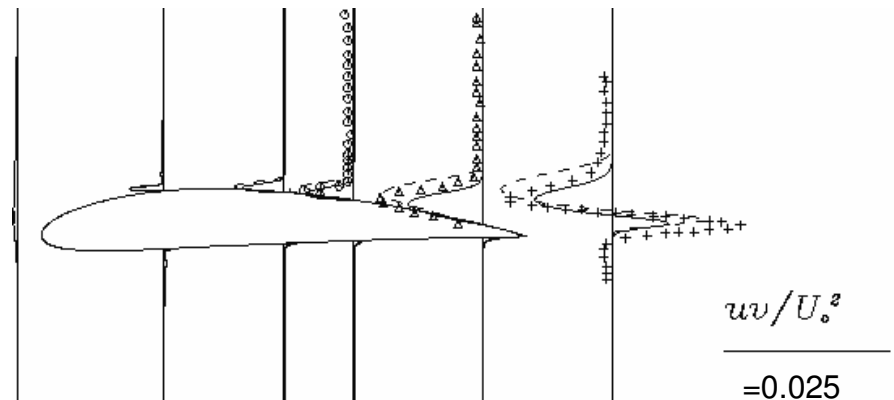
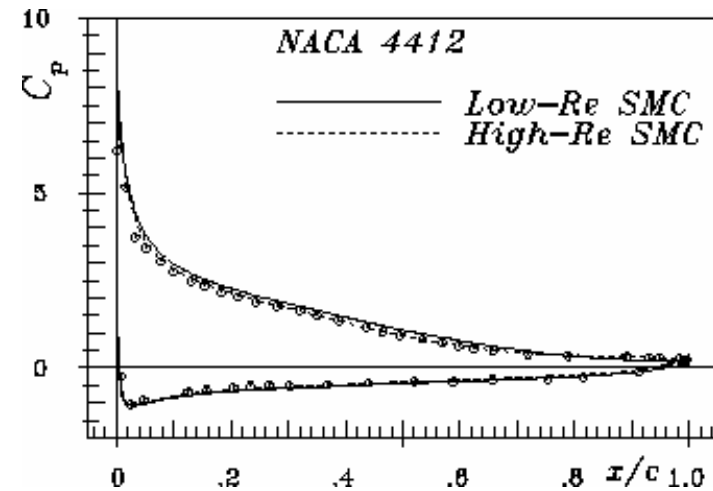
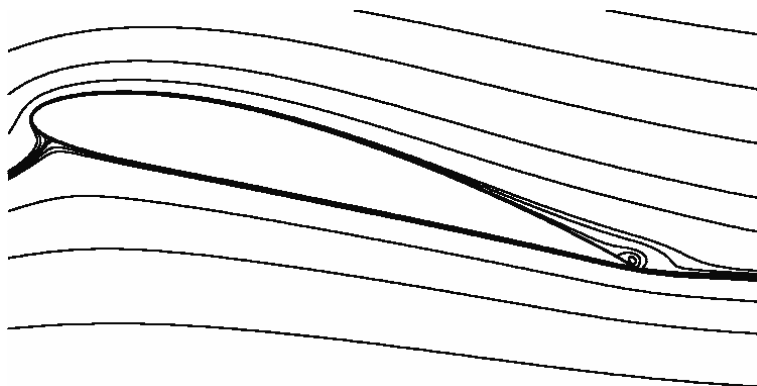


Subsonic flow around an airfoil*

GL high-Re SMC

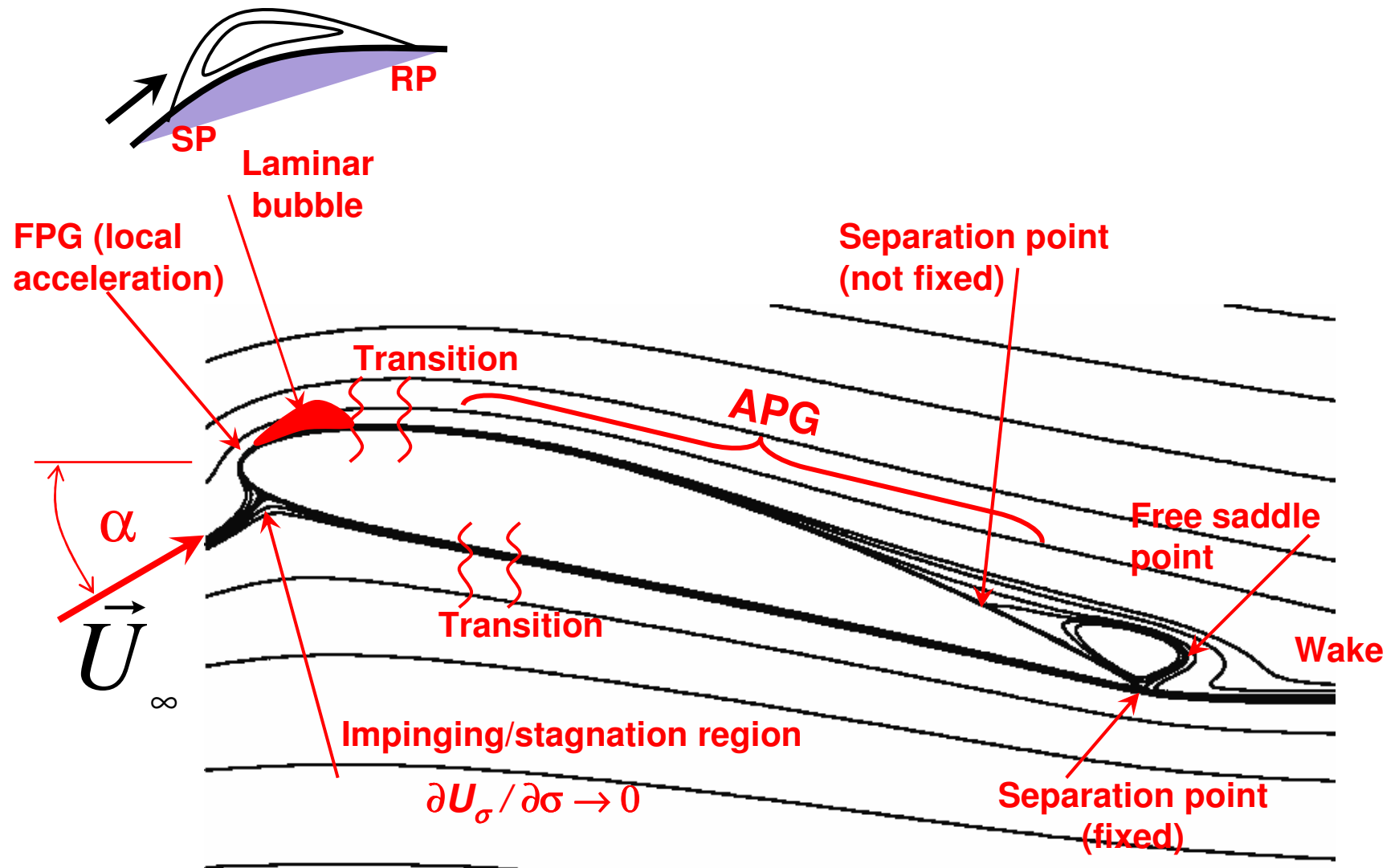


HJ low-Re SMC



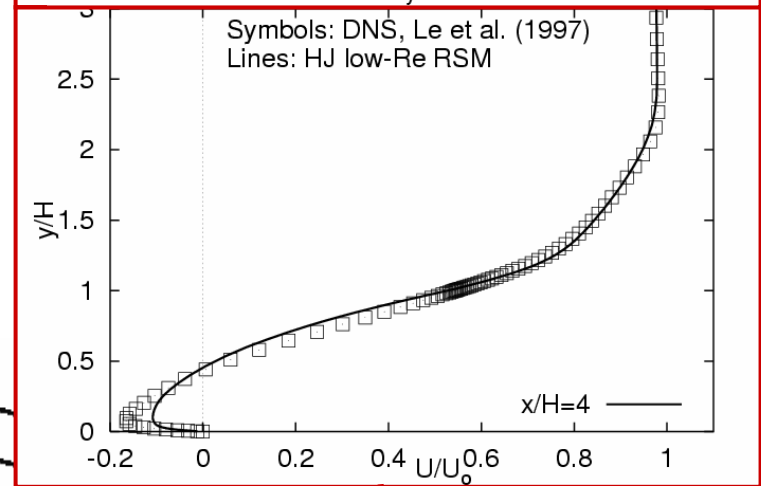
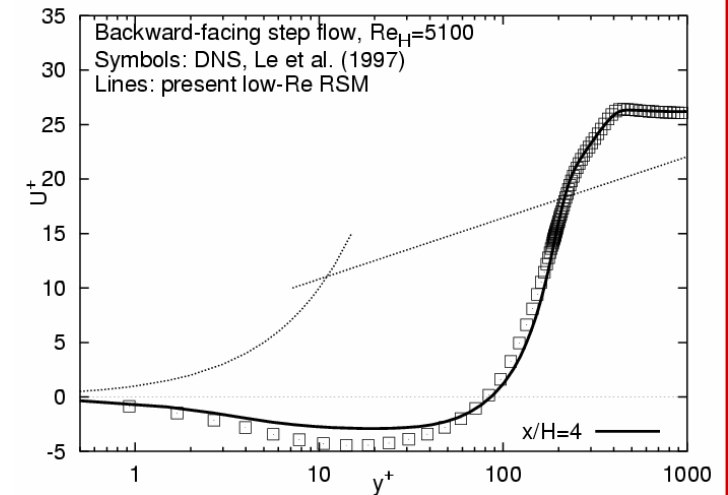
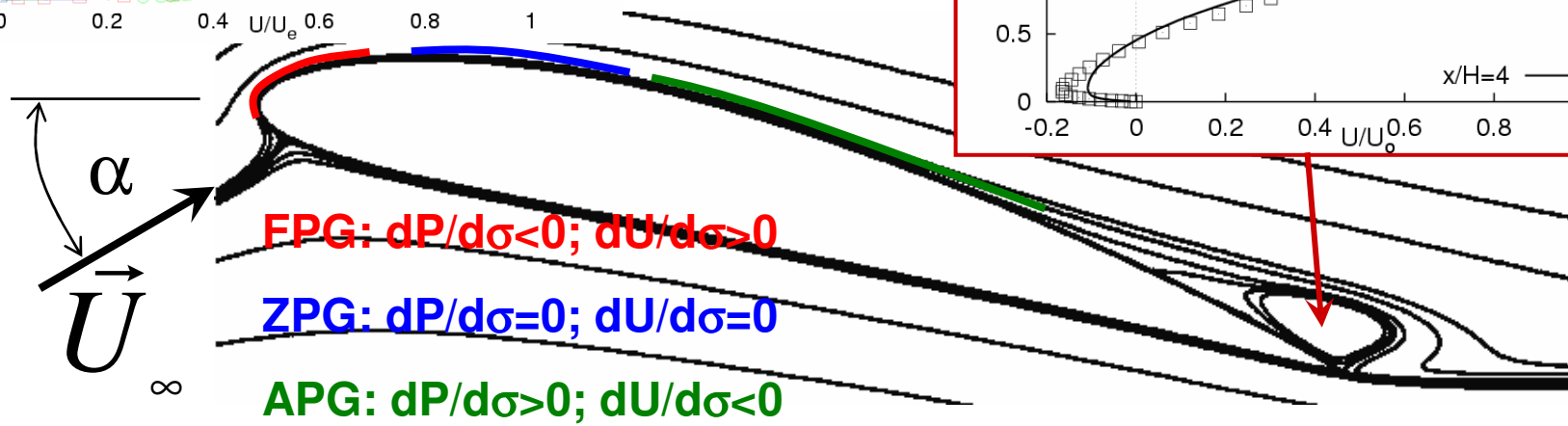
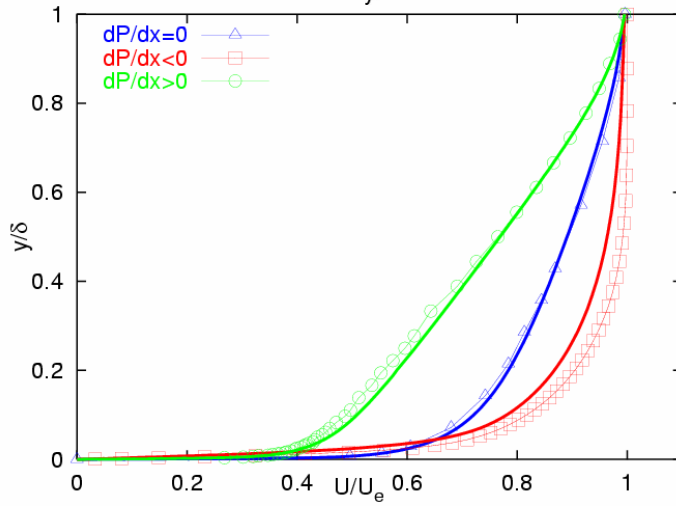
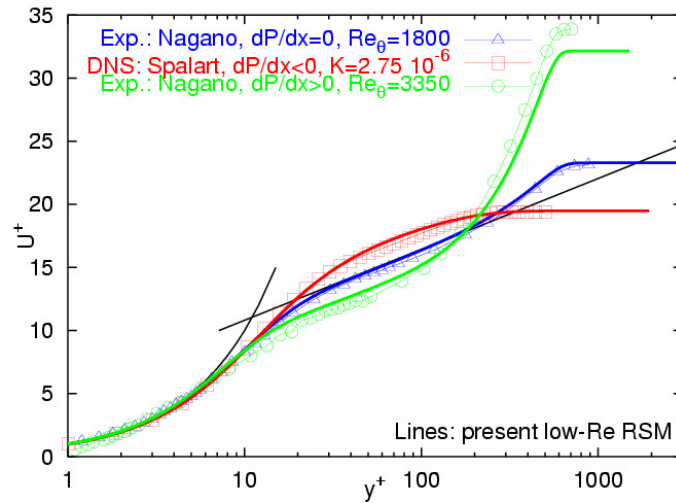
*Jakirlic, S., Hadzic, I., Djugum, A., and Tropea, C. (2002): Boundary-Layer separation Computed by Second-Moment Closure Models. *Notes on Numerical Fluid Mechanics*, Vol. **77**, pp. 215-222, Springer Verlag

Subsonic flow past an airfoil configuration: flow characteristics/topology



• Possible relaminarization at very high Reynolds numbers

Model validation: test cases



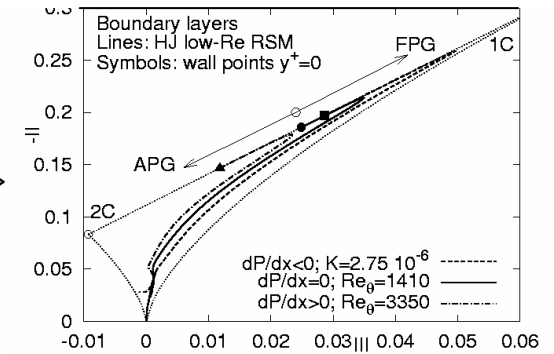
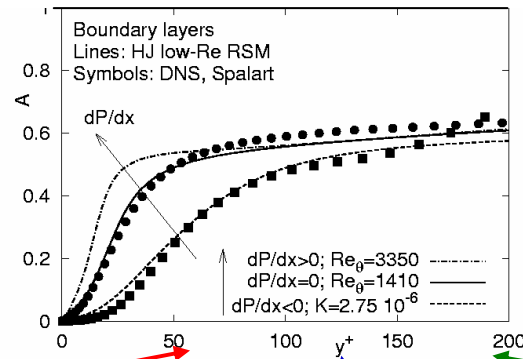
Model validation: test cases

FPG: $dP/d\sigma < 0$; $dU/d\sigma > 0$

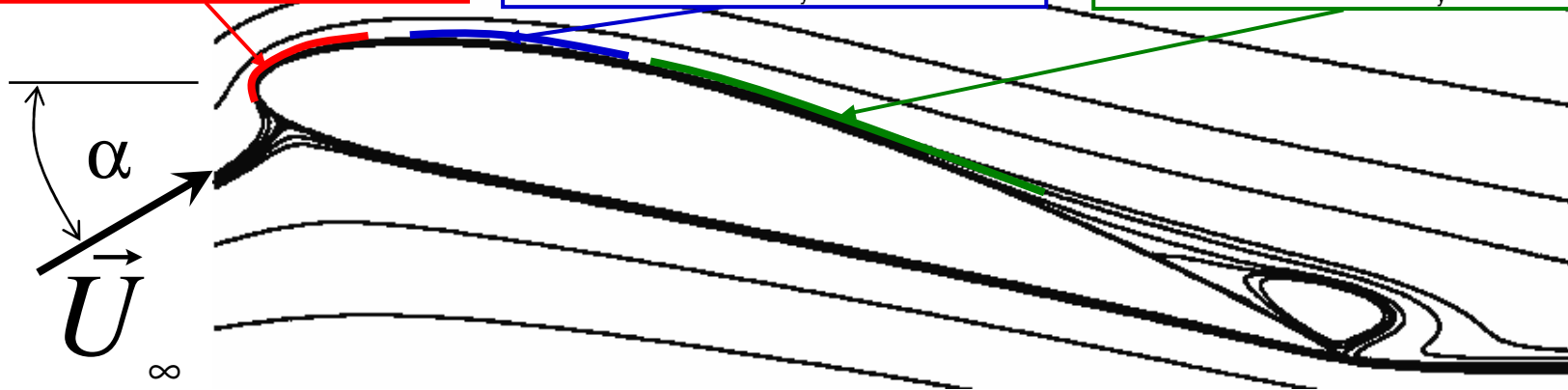
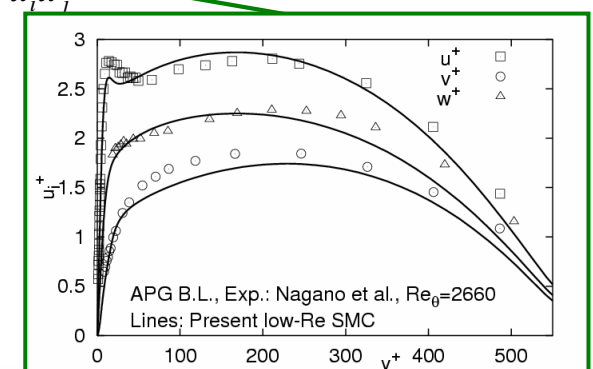
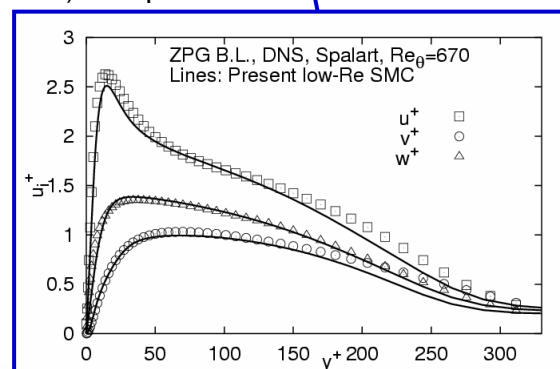
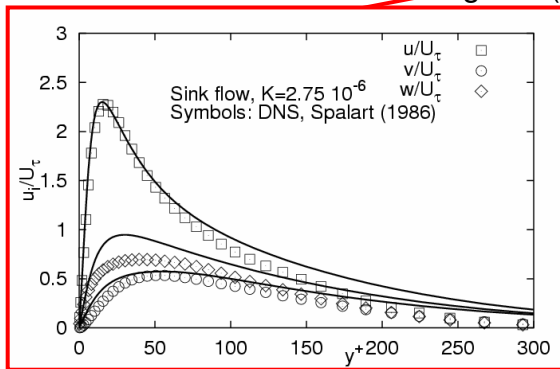
ZPG: $dP/d\sigma = 0$; $dU/d\sigma = 0$

APG: $dP/d\sigma > 0$; $dU/d\sigma < 0$

Re-stress anisotropy parameters



Diagonal (normal) components of the Re-stress tensor $u_i u_i$



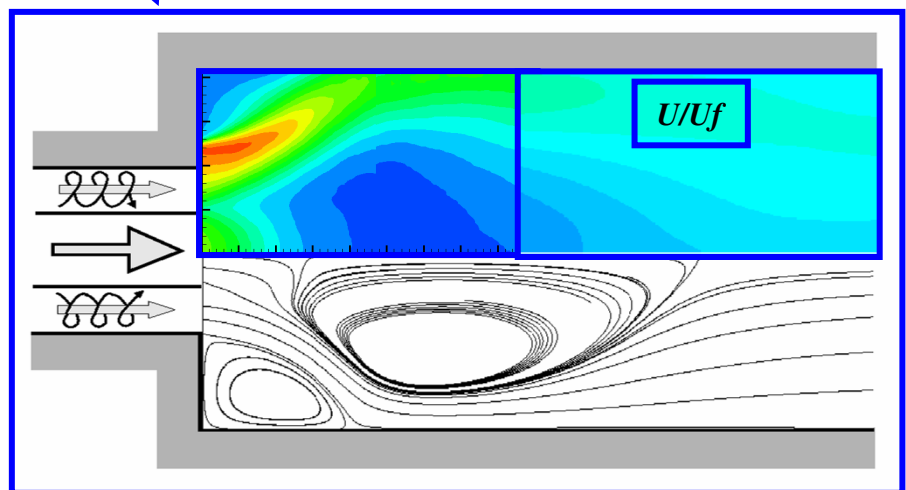
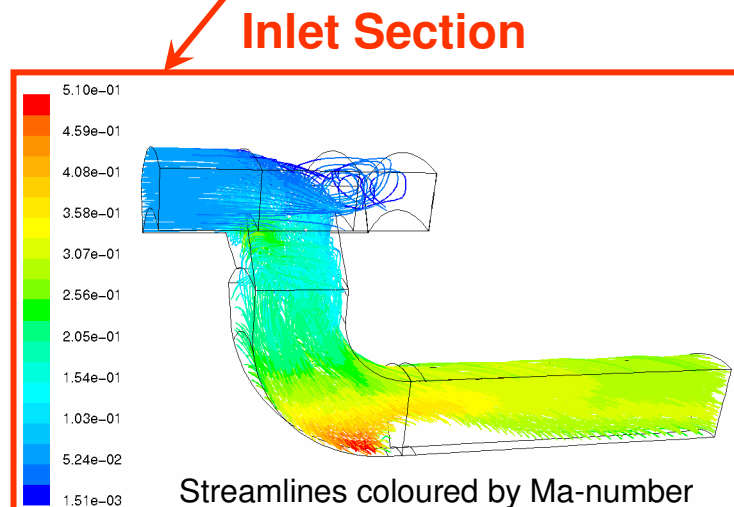
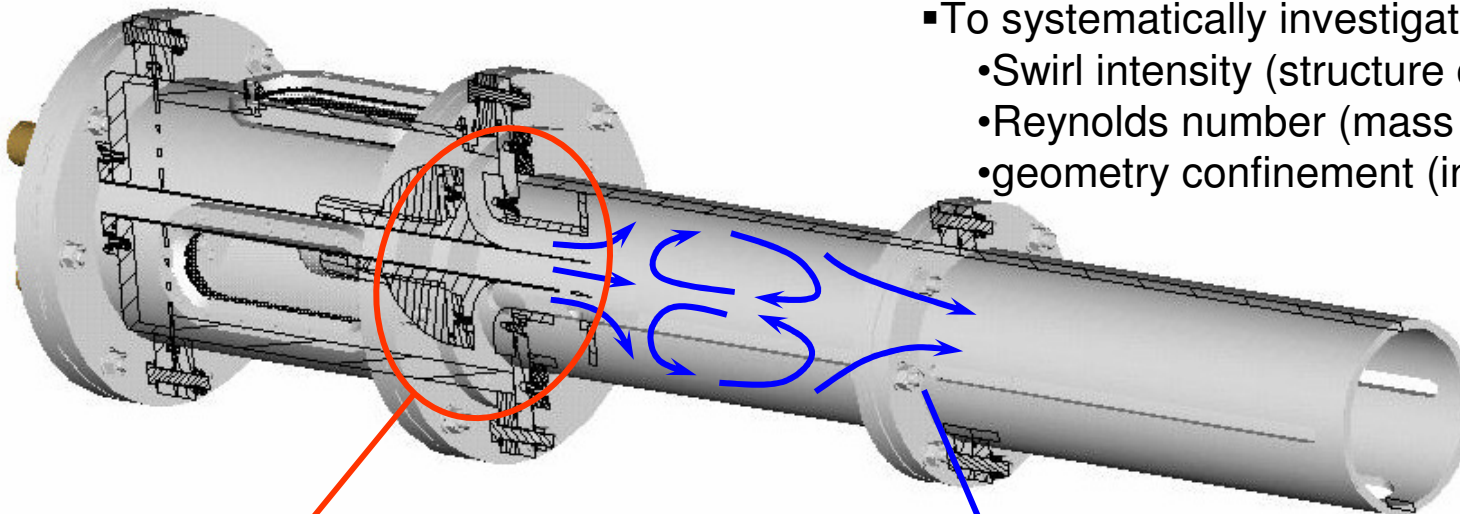
Flow examples

- Experimental and numerical investigations of flow and mixing in a swirl combustor
- Single drop impact onto dry (wetable and non-wetable) surfaces
- Inner flow field in a flat fan pressure atomizers

Single turbo-annular model combustor

BMBF Project: “**Experimental and numerical investigations of flow and mixing in a swirl combustor**”

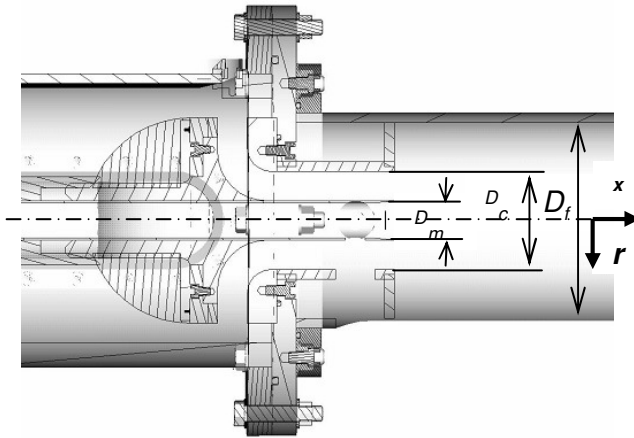
- To systematically investigate the effects of
 - Swirl intensity (structure of swirling inflow)
 - Reynolds number (mass flow rate ratios)
 - geometry confinement (in terms of ER)



Objective

- To systematically investigate effects of
 - swirling inflow structure
 - circumferential velocity type (both configurations with annular and central swirling jets were considered)
and
 - swirl intensity (S)
 - geometry confinement (in terms of ER)on flow and mixing in model combustor
- Modelling strategy:
 - analysis (also „*a priori*“) of existing (SMC) model schemes with respect to flow phenomena appearing in combustion chambers (recirculation, swirling)

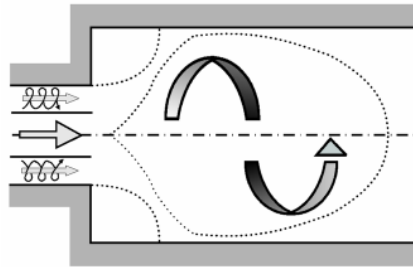
Working conditions



<i>Identification of the Tube</i>	<i>Inner (D_i)/outer (D_o) Diameter</i>
Non-swirling main flow	36 mm/40mm
Swirling coaxial flow	40mm/100 mm
Flue (ER=2)	200 mm
Flue (ER=1.5)	150 mm

<i>Parameter</i>	<i>Range</i>
Reynolds number (Main flow)	$22.500 \leq Re_m \leq 112.750$
Mass flow rate (Main flow)	$0,01 \text{ kg/s} \leq m \leq 0,05 \text{ kg/s}$
Reynolds number (Annular flow)	$49.530 \leq Re_c \leq 132.100$
Mass flow rate (Annular flow)	$0,1 \text{ kg/s} \leq m \leq 0,25 \text{ kg/s}$
Swirl intensities	$0 \leq S \leq 1,2$
Expansion ratio	1,5 und 2,0

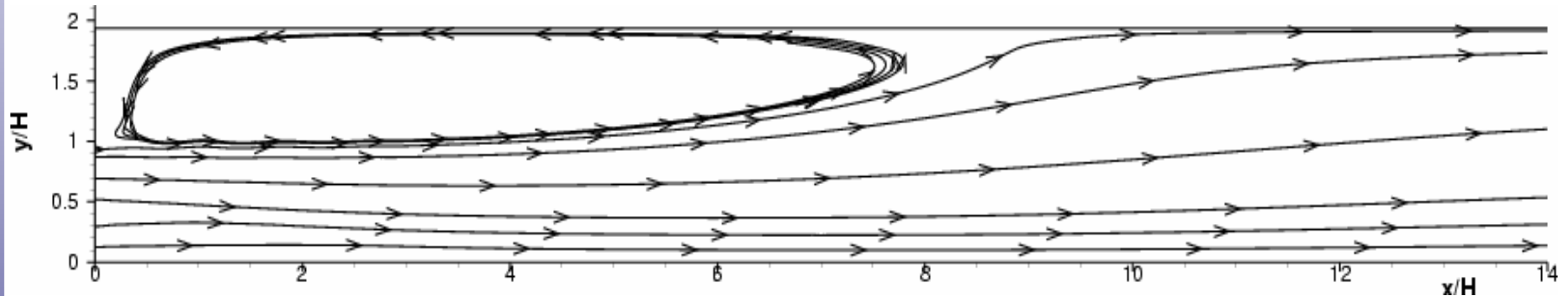
Roback & Johnson's single annular gas combustor: without and with swirl



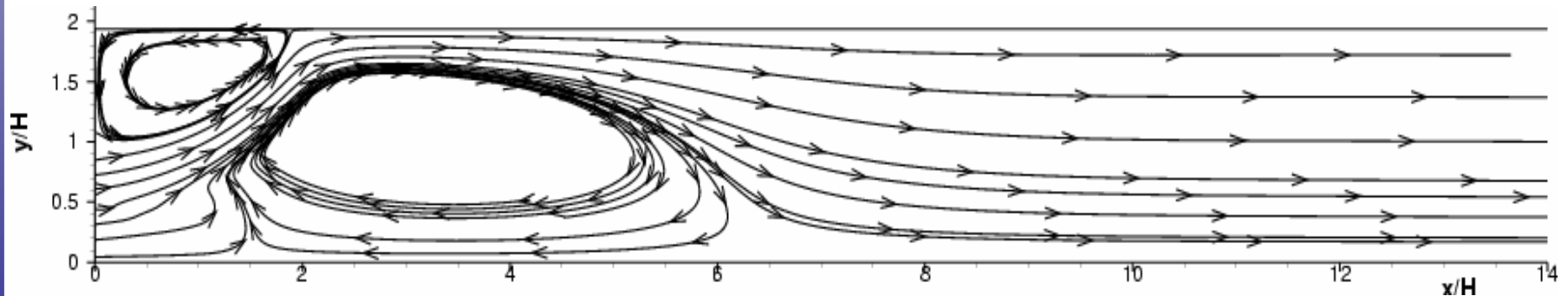
→w.o. swirl

- $ER=2.1$
- $S=0.40$ & 0.41
- $Re=47.500$
- Mixing ($\rho = \text{const}$)

- **LES** (no swirl): Akselvol & Moin (1996)
- **LES** (swirl): Pierce & Moin (1998)

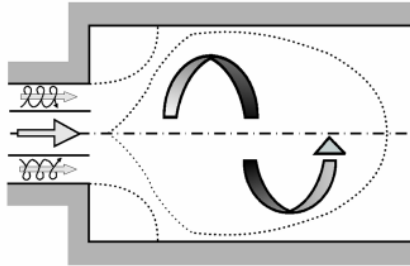


→with swirl



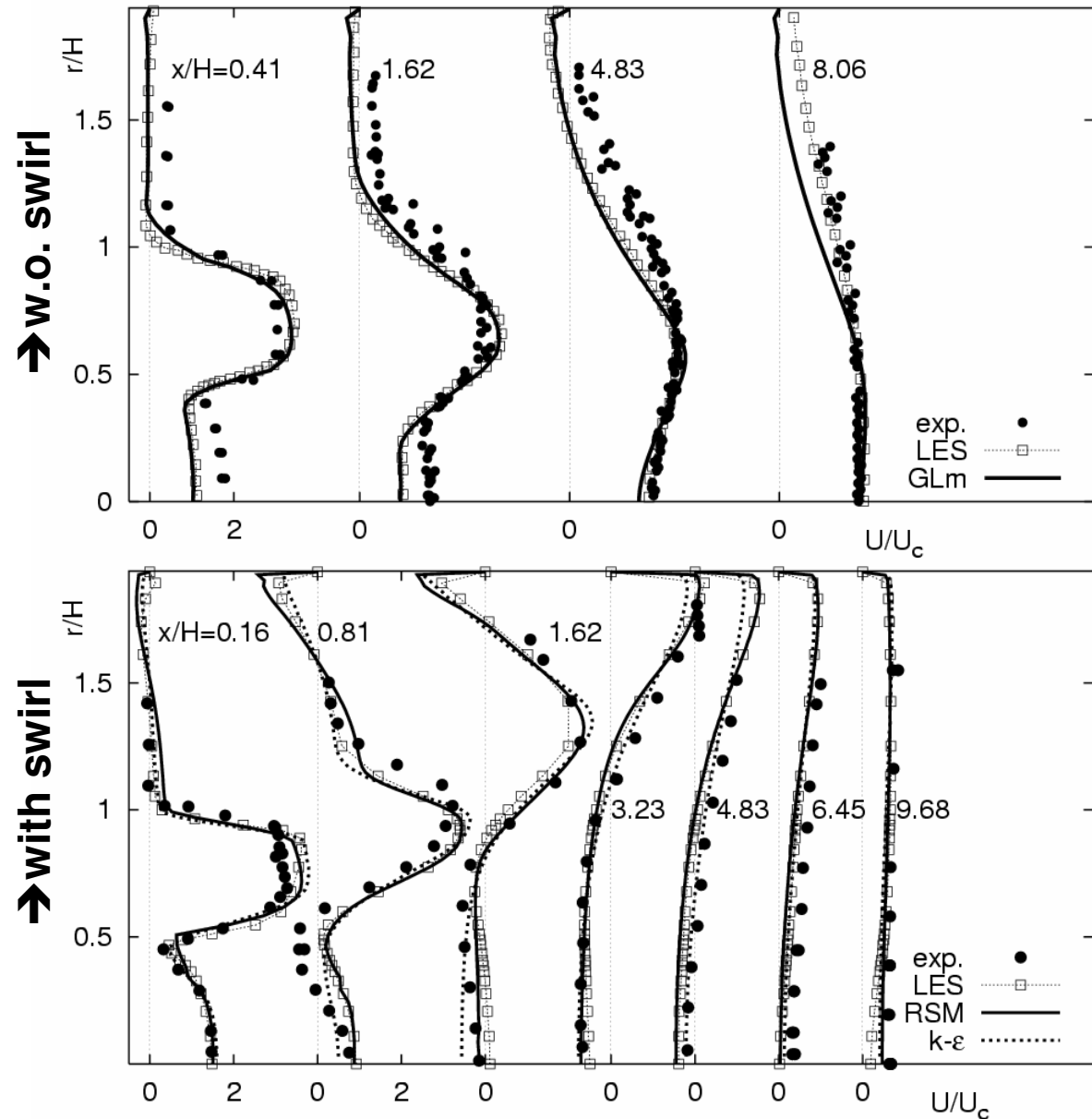
- Complex mean strain tensor: mean and secondary shearing, streamline curvature (local & swirl/transverse), a.p.g. effects, Re-stress anisotropy

Roback & Johnson's single annular gas combustor without and with swirl: U - velocities

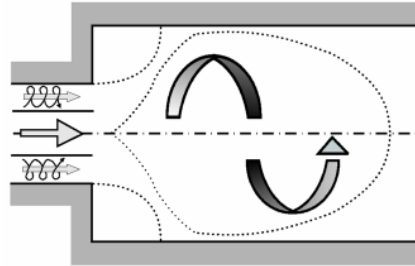


- $ER=2.1$
- $S=0.0$ & 0.41
- $Re=47.500$
- Mixing ($\rho = \text{const}$)

- **LES** (no swirl):
Akselvol & Moin
(1996)
- **LES** (swirl):
Pierce & Moin
(1998)



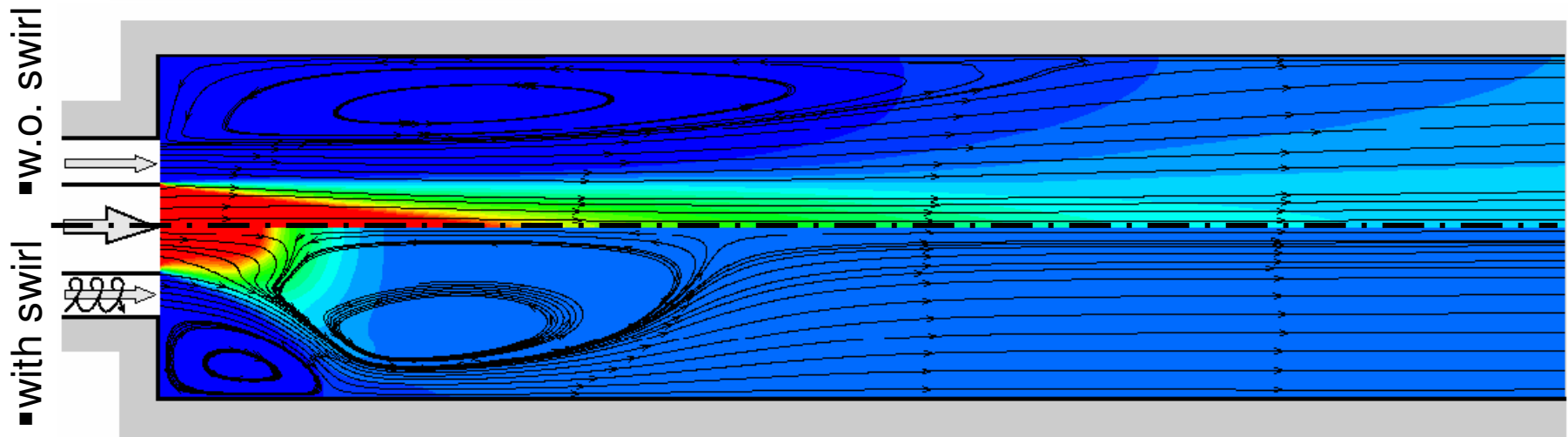
Roback & Johnson's single annular gas combustor, scalar transport without and with swirl: mean concentration



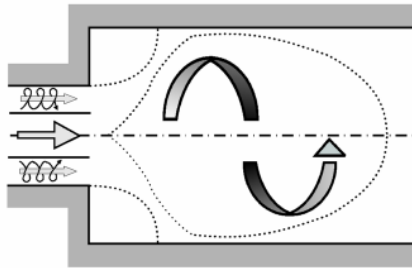
- $ER=2.1$
- $S=0.0$ & 0.41
- $Re=47.500$
- Mixing ($\rho = \text{const}$)

- **LES** (no swirl):
Akselvol & Moin
(1996)
- **LES** (swirl):
Pierce & Moin
(1998)

Mixture Fraction F ■ $F=1$ ■ $F=0$



Roback & Johnson's single annular gas combustor, scalar transport without and with swirl: mean concentration



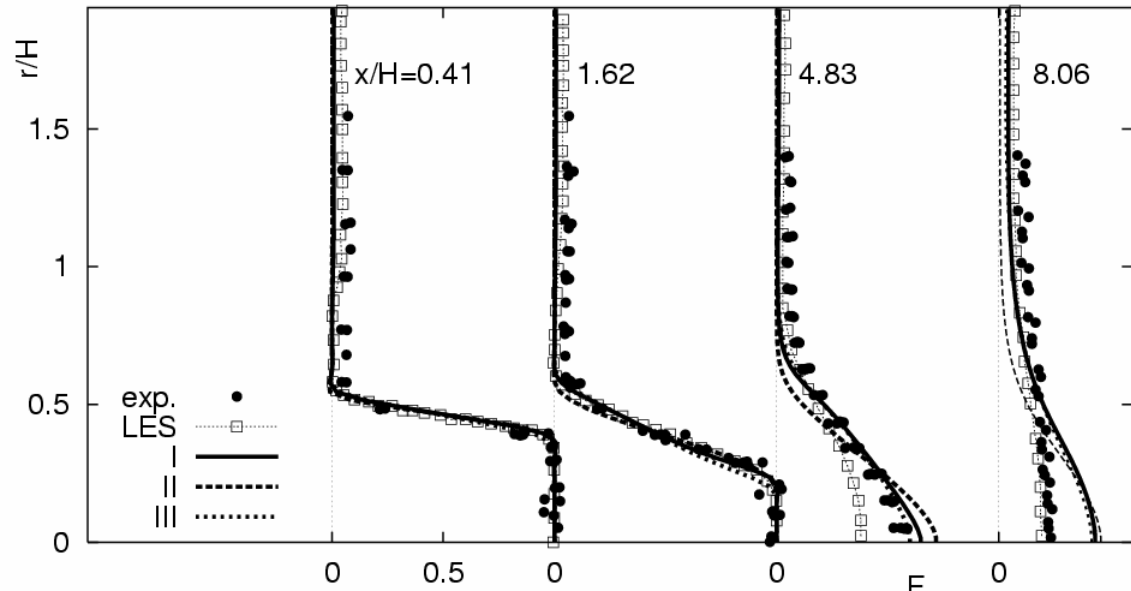
- $ER=2.1$
- $S=0.0$ & 0.41
- $Re=47.500$

➤ Mixing ($\rho = \text{const}$)

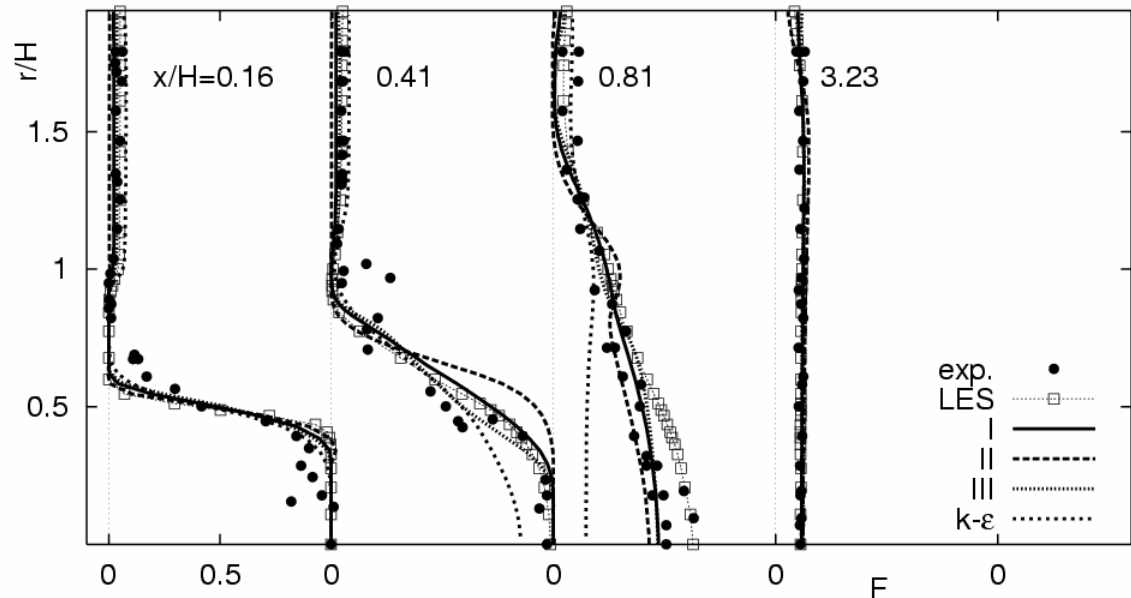
▪ **LES** (no swirl):
Akselvol & Moin
(1996)

▪ **LES** (swirl):
Pierce & Moin
(1998)

➔ w.o. swirl



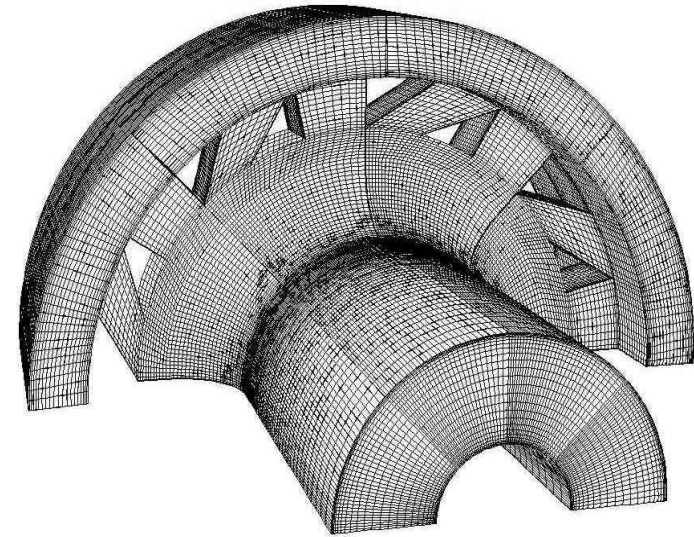
➔ with swirl



RANS (SMC) computations: swirl generator system and input pipe

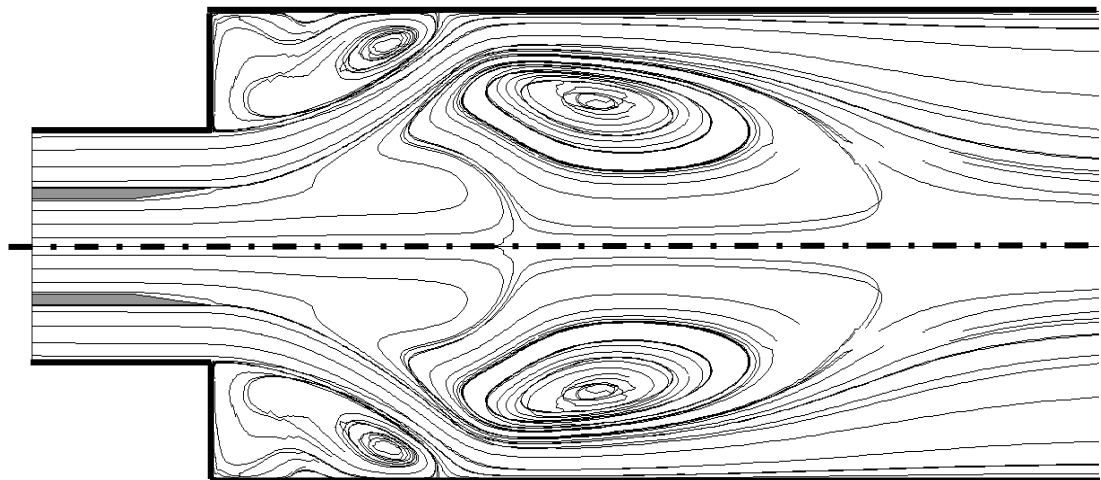
→ 3-D computations (FLUENT) of the inlet section including swirl generator system

- One eighth of the configuration was accounted for (the inlet section including swirl generator system was meshed by 150.000 cv's)
- Periodic inlet/outlet in the azimuthal direction; pressure b.c. at the outlet
- Flow in the flue was computed under simplified conditions of axisymmetry

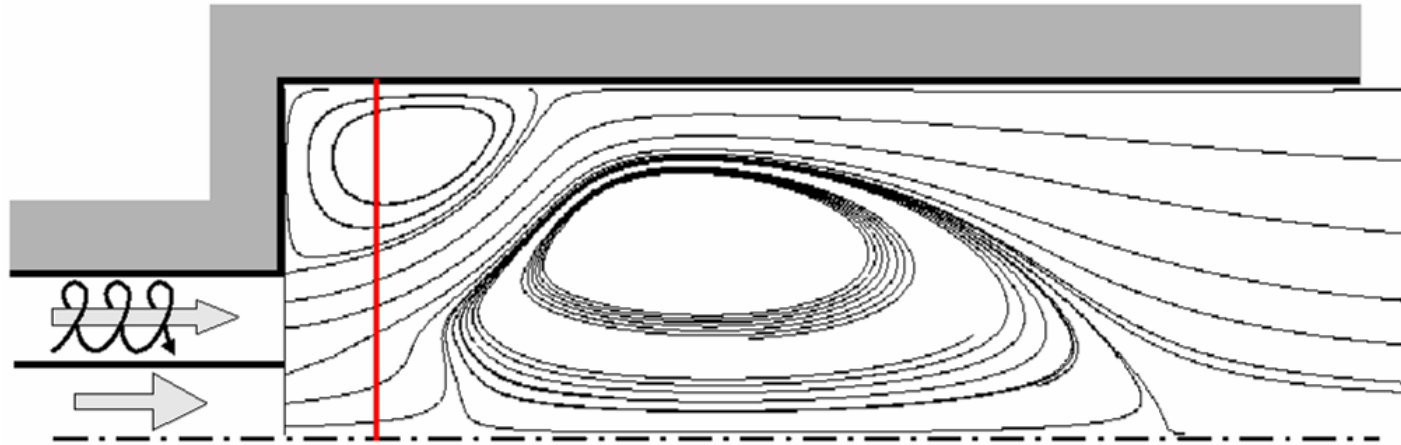


$S=0.6$

- GL RSM (with wall reflection term) + variable model coefficients (near-wall RSM, Launder & Shima) + enhanced wall treatment (a two-layer treatment based on the 1-eq. $k-\epsilon$ model)

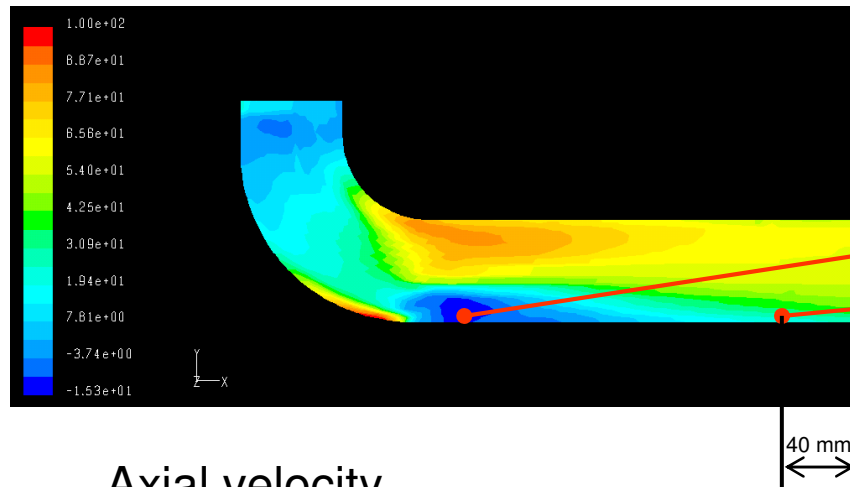


Motivation: swirling inflow conditions

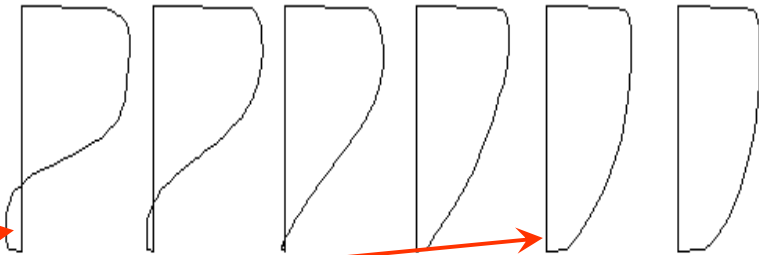


- First experimental cross-section (combustor interior) coincides commonly with inlet section of the computational domain →
- inlet section is positioned within recirculation zones (side walls are neglected → the adverse pressure gradient effect – geometry expansion - can be not accounted for),
- discretization of swirling devices leads to a highly demanding 3-D calculation.
- Idea/Solution → Inflow data generated computationally! (?)

RANS (SMC) computations: swirl generator system and input pipe

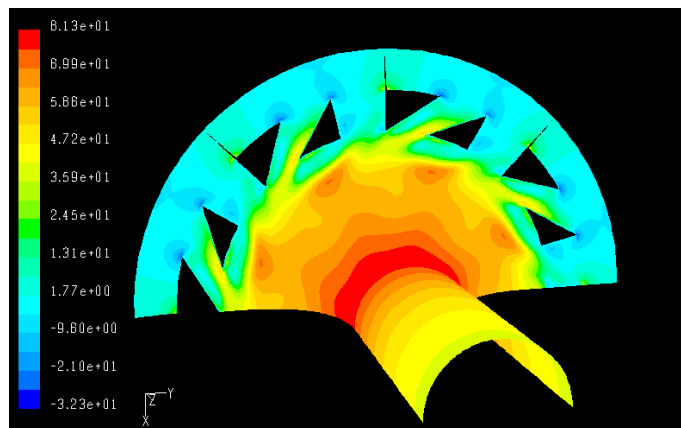


Axial velocity

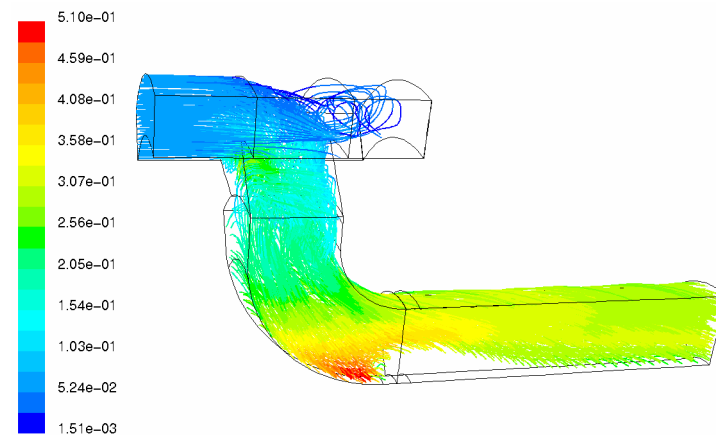


↑
Inlet data for
combustion
chamber

Re=345.205 (mass flow rate=0.5 kg/s); S=1.2

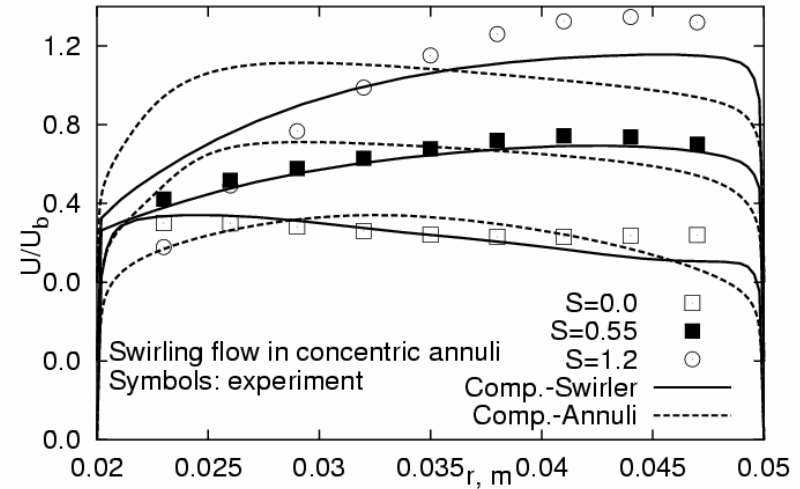
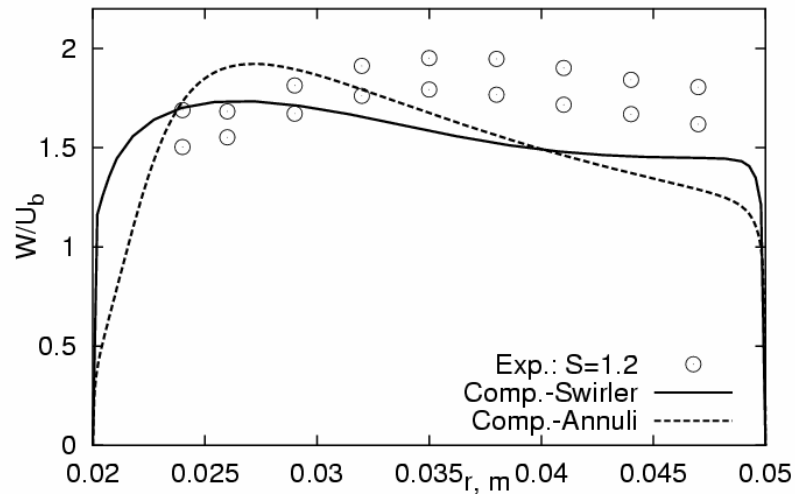


Circumferential velocity

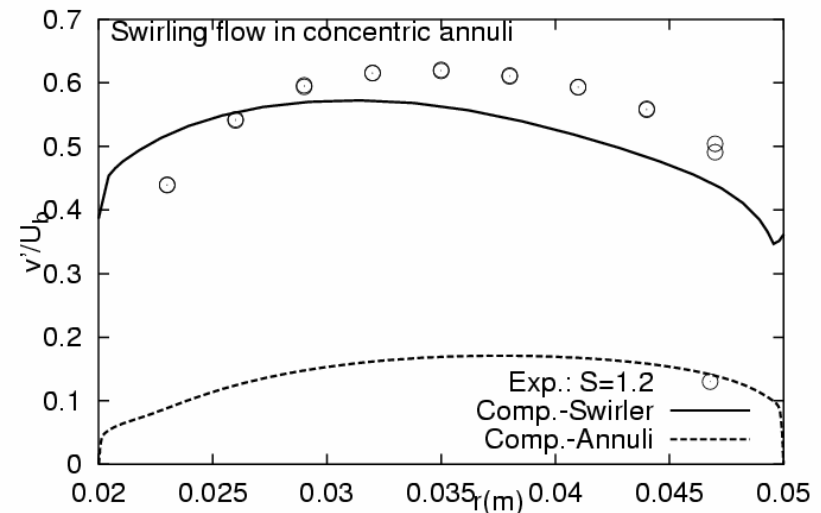
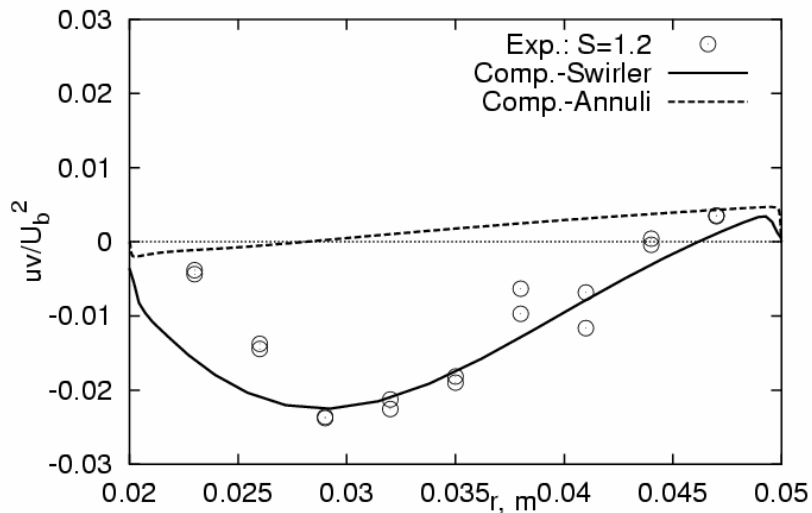


Streamlines coloured by Ma-number

RANS (SMC) computations: swirl generator system and input pipe



Circumferential velocity profiles for the case with strongest swirl and axial velocity profile for range of the swirl numbers (right)



Shear and wall-normal stresses in the concentric annulus of the inlet section of the present model combustor for the case with strongest swirl

Experiment vs. RANS (SMC) computations: axial velocities

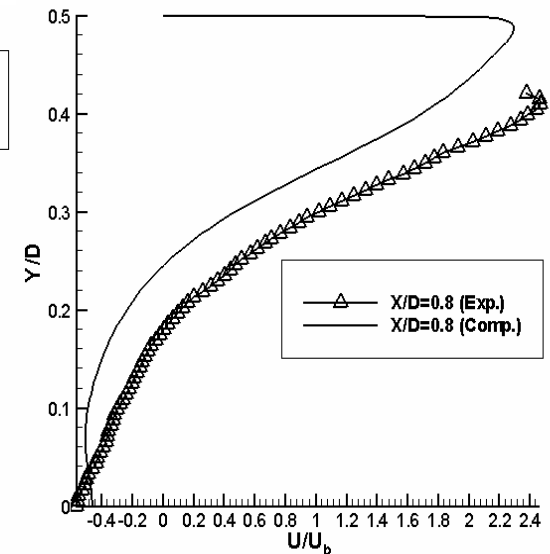
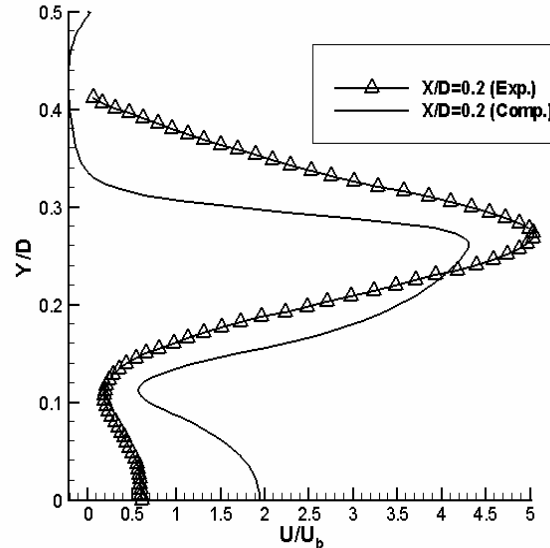
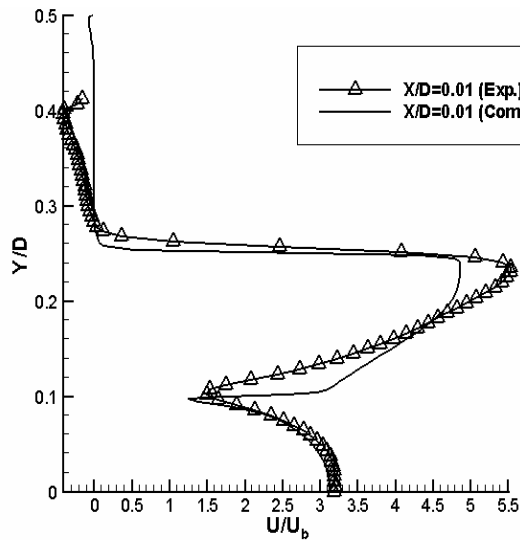
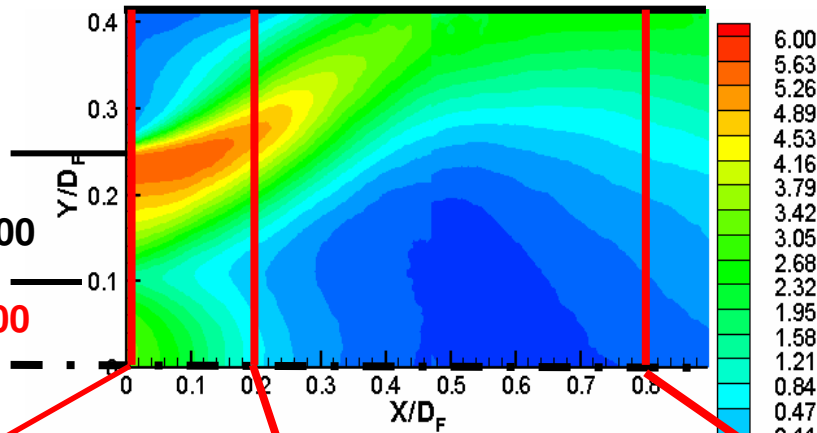
U/U_f

$U_c/U_f=4.3$,
 $U_m/U_f=2.6$,
 $D_f/D_c=2$,
 $D_f/D_m=5.6$

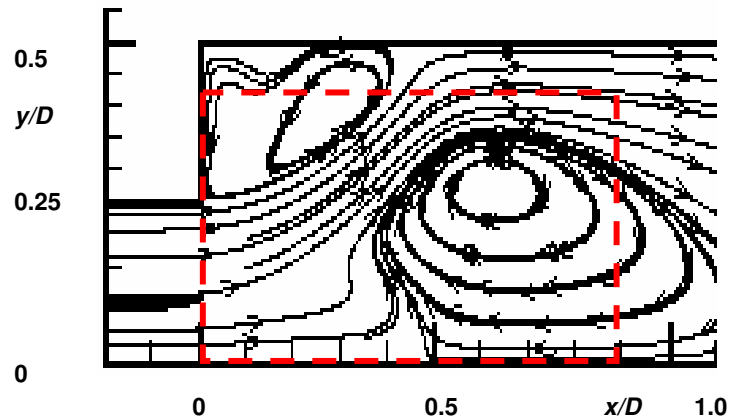
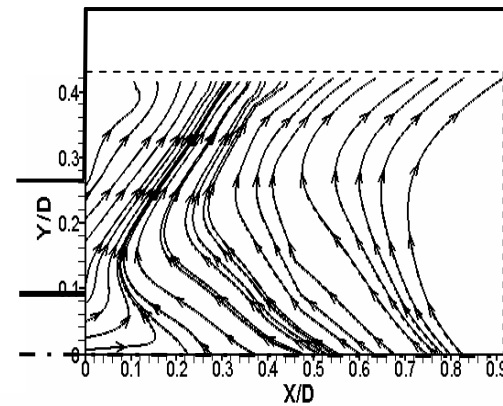
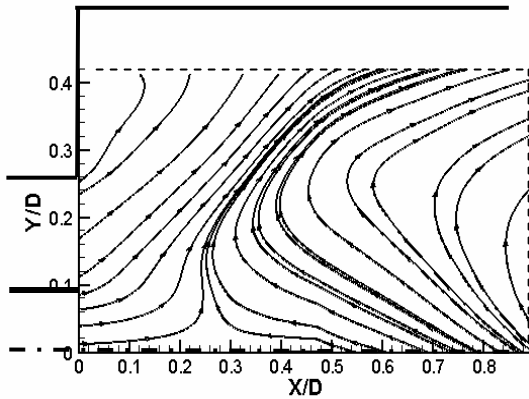
$S=0,6$

$Re_c=125.500$

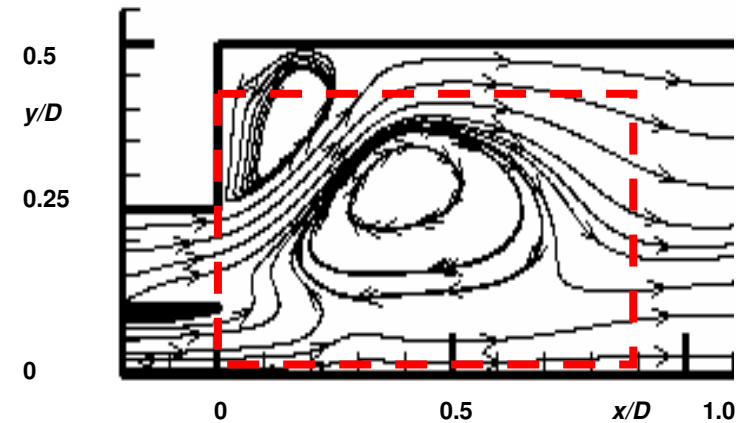
$Re_m=47.000$



Experiment vs. RANS (SMC) computations: streamline patterns



$S=0.6$

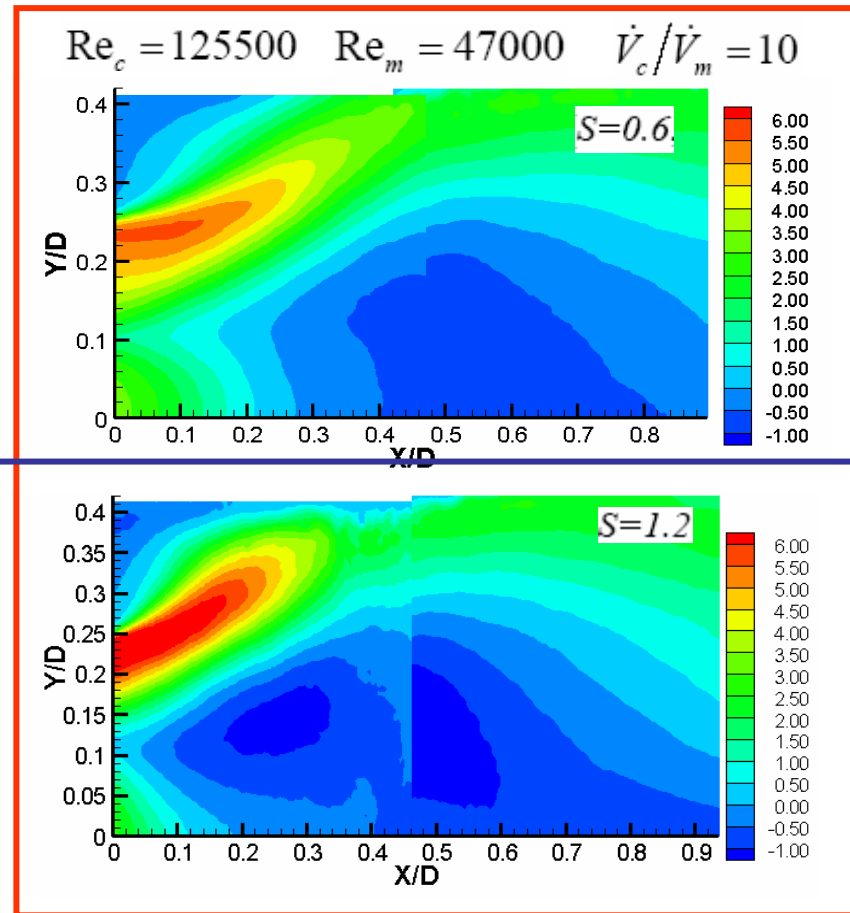


$S=1.2$

Outlook

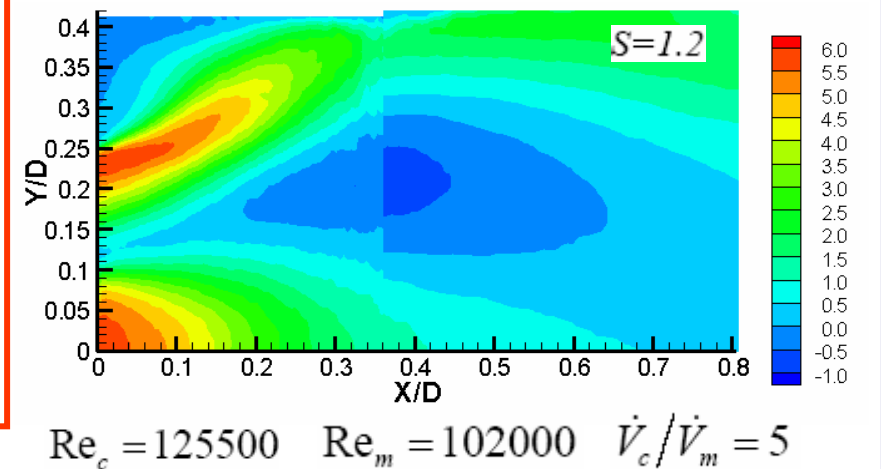
■ Swirling flow within the flue:

⇒ Flow and mixing in a swirl combustor model, Exp.: Palm et al.
(Chair of Fluid Mechanics and Aerodynamics, TU Darmstadt)



■ Swirl intensity influence

■ Volume rate ratio influence

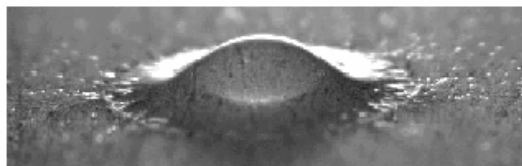


Experimental and numerical drop impact on solid dry surfaces

Some possible outcomes



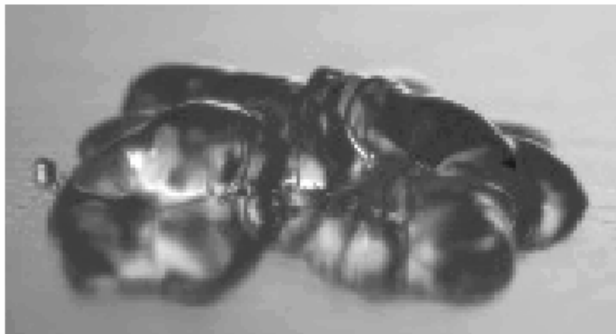
Deposition



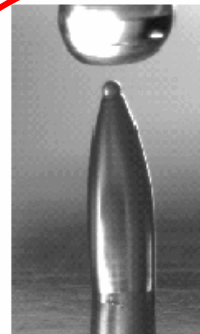
Prompt splash



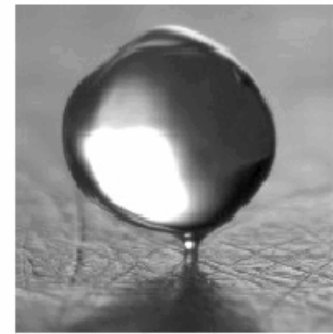
Corona splash



Receding break-up



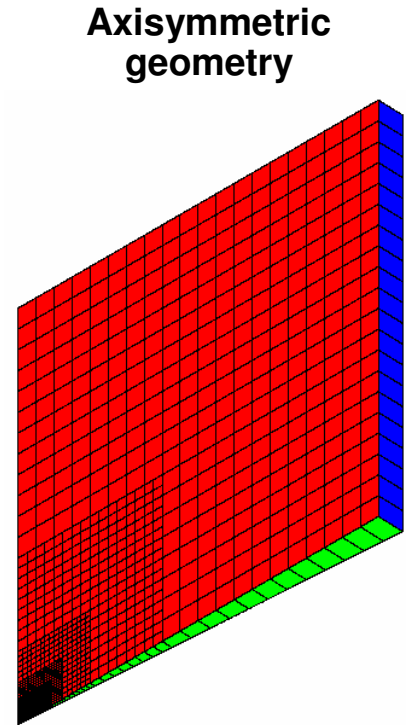
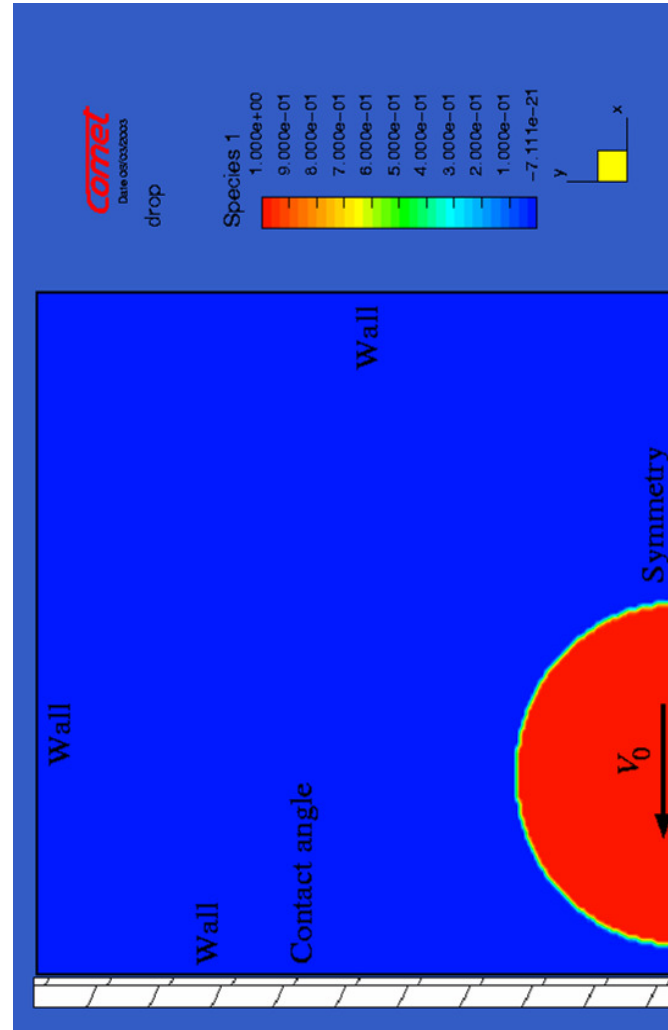
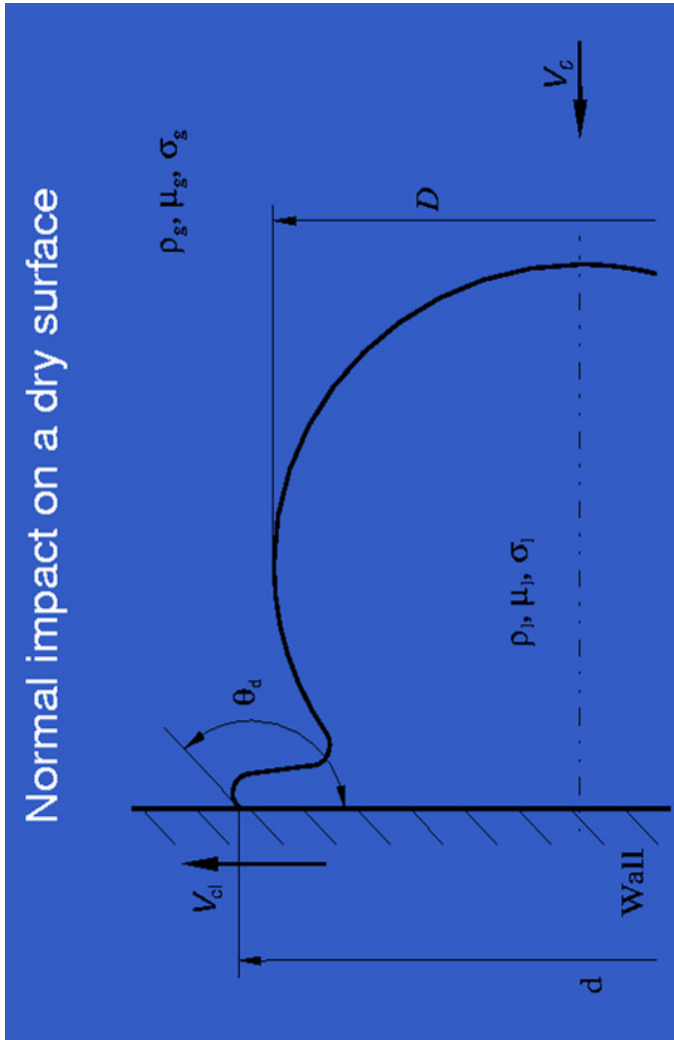
Partial rebound



Rebound

Numerical drop impact on solid dry surfaces

Schematic of the cases considered



Modelling: Mathematical description (1)

Mass conservation

$$\frac{d}{dt} \int_V \rho dV + \int_S \rho \vec{v} \cdot \vec{n} ds = 0$$

Momentum balance

$$\frac{d}{dt} \int_V \rho \vec{v} dV + \int_S \rho \vec{v} (\vec{v} \cdot \vec{n}) ds = \int_S (\vec{n} \cdot \mathbf{T}) ds + \int_V (\vec{f}_b + \vec{f}_\sigma) dV$$

Volume concentration balance

$$\frac{d}{dt} \int_V C dV + \int_S C (\vec{v} \cdot \vec{n}) ds = 0$$

+ boundary conditions

with

C : Volume concentration

ρ : Density

\vec{v} : Velocity

V : Control volume

S : Surface of control volume

\vec{n} : Normal to the surface

$$\mathbf{T} = -p \mathbf{I} + \mu [(\nabla \vec{v}) + (\nabla \vec{v})^T]$$

μ is the viscosity

\mathbf{I} is unity matrix

p is the pressure

\vec{f}_b are body forces

\vec{f}_σ are surface tension equivalent forces

Numerical drop impact on solid dry surfaces

- Finite volume method
- VOF (Volume-of-Fluid) related surface capturing method:

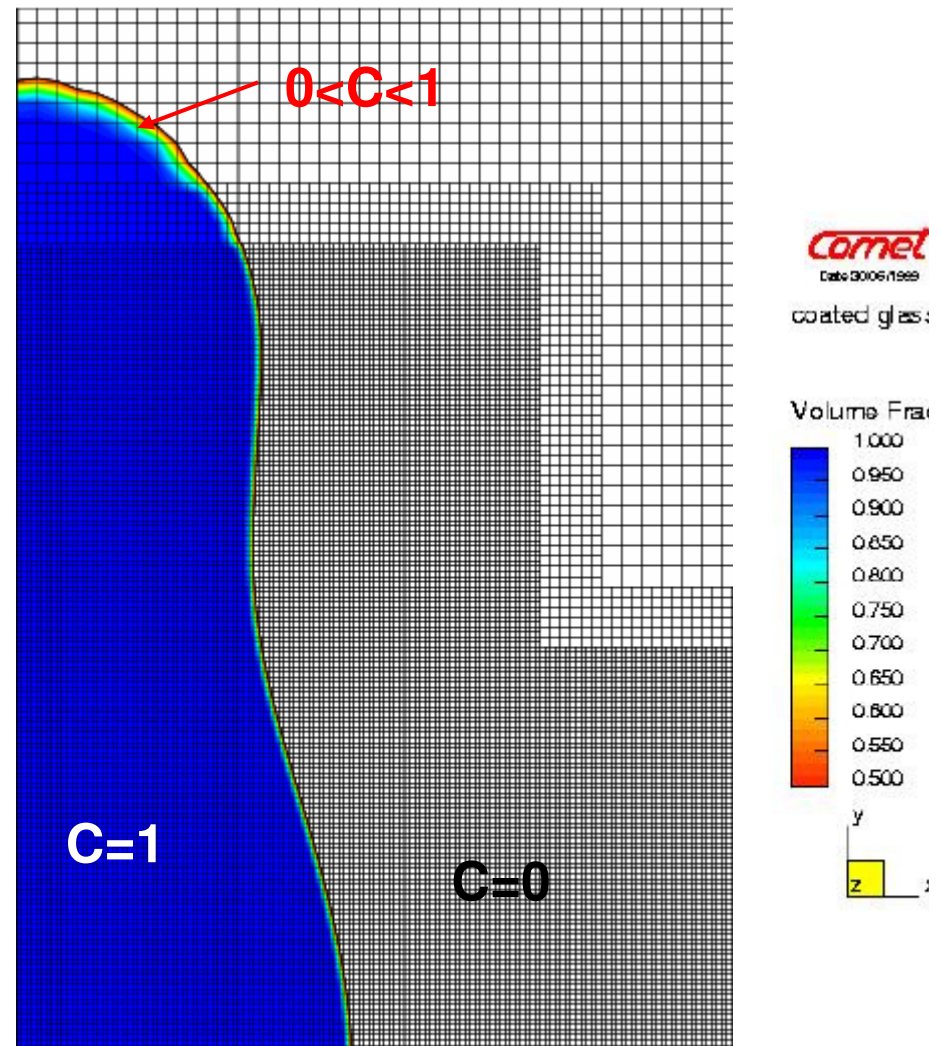
→ Effective density $\rho = C\rho_1 + (1-C)\rho_0$
 Effective viscosity $\mu = C\mu_1 + (1-C)\mu_0$
 Surface tension σ

$$C(\mathbf{x}, t) = \begin{cases} 0 & \text{fluid 0 (gas)} \\ 0 < C < 1 & \text{transition area} \\ 1 & \text{fluid 1 (liquid)} \end{cases}$$

→ HRIC – High Resolution Interface Capturing

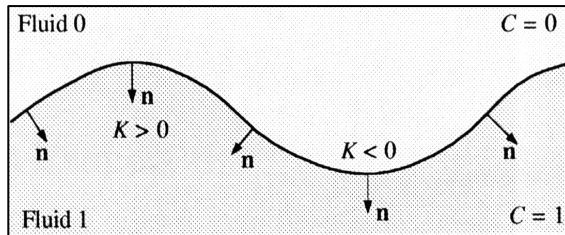
→ Continuum surface method (free surface tension force)

→ Variable contact angle (Hoffman law)



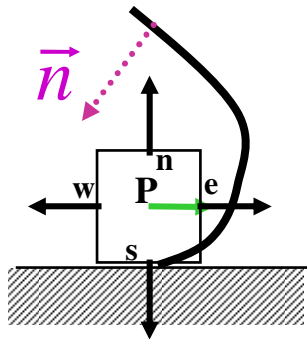
Modelling: Mathematical description (2)

Surface tension force on the liquid/gas interface

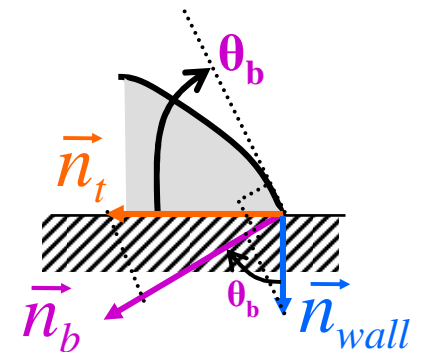


$$\vec{f}_\sigma = -\sigma \left[\vec{\nabla} \cdot \left(\frac{\vec{\nabla} C}{|\vec{\nabla} C|} \right) \right] \vec{\nabla} C = -\sigma K \vec{\nabla} C \quad \left(\vec{n} = \frac{\vec{\nabla} C}{|\vec{\nabla} C|} \right)$$

K is the curvature



$$\vec{\nabla} C = \frac{1}{V} \oint_S C \, d\vec{S}$$



$$\vec{n}_b = \left(\frac{\vec{\nabla} C}{|\vec{\nabla} C|} \right)_b = \vec{n}_{wall} \cos(\theta_b) + \vec{n}_t \sin(\theta_b)$$

\vec{n}_{wall} : Normal to the wall vector

\vec{n}_t : Parallel to the wall vector

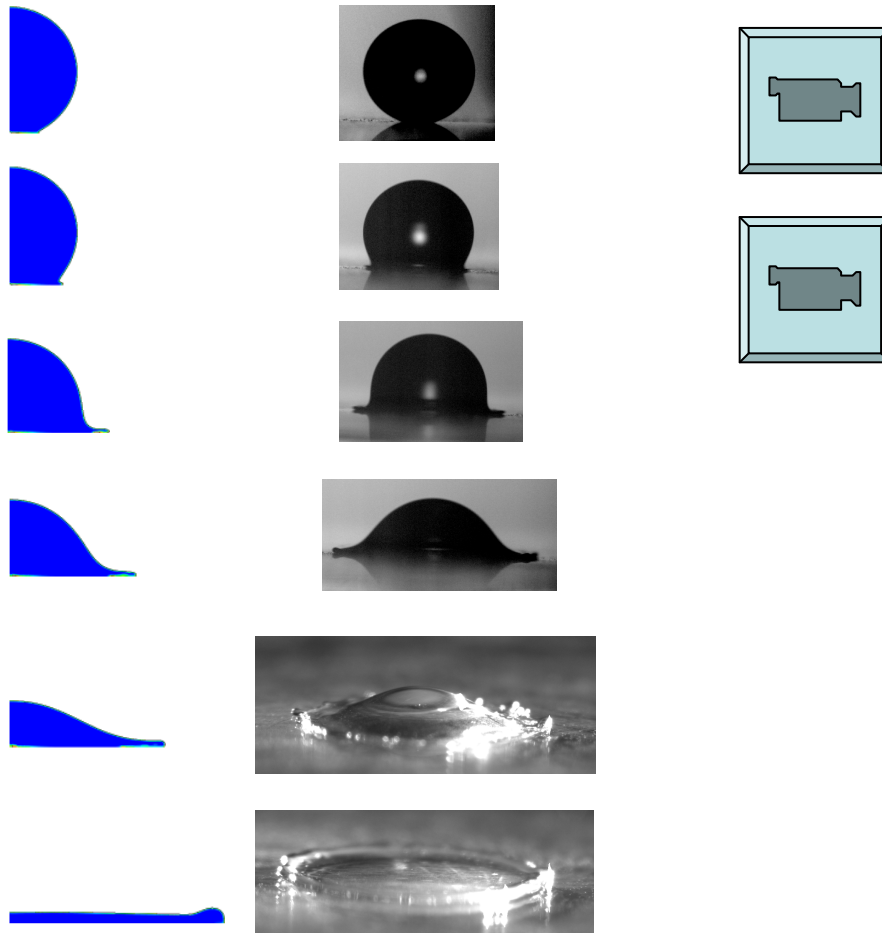
Constant ($\Theta_d = \Theta_o$) vs. variable Θ_d

- Hoffman law:

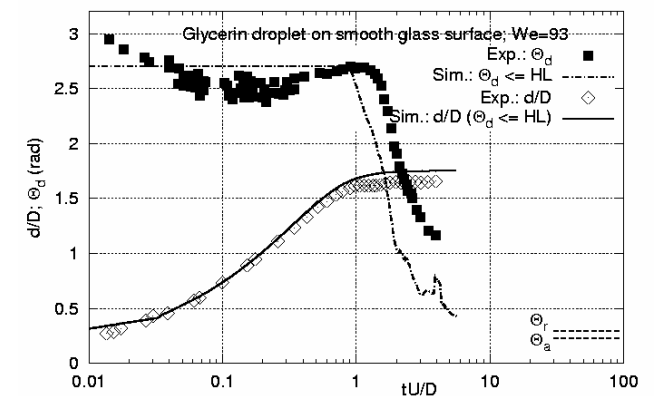
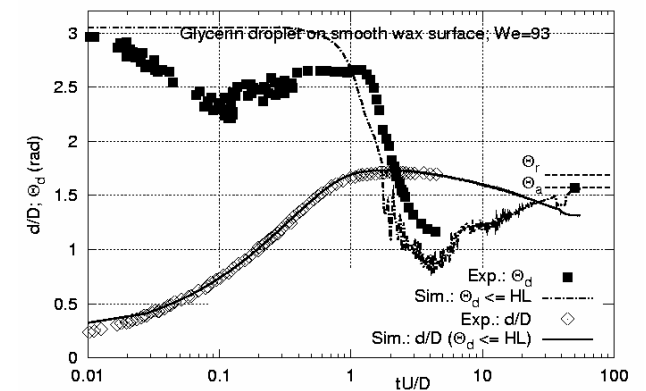
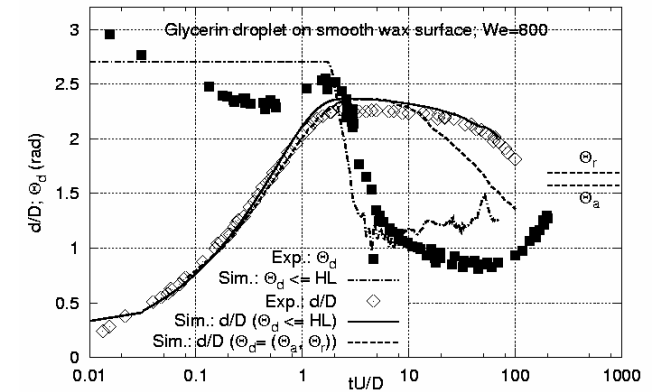
$$\Theta_d = f_{Hoff} \left[Ca + f_{Hoff}^{-1} (\Theta_o) \right]; \quad Ca = \frac{\mu V_{CL}}{\sigma}$$

$$f_{Hoff}(x) = \arccos \left\{ 1 - 2 \tanh \left[5.16 \left(\frac{x}{1 + 1.31x^{0.99}} \right)^{0.76} \right] \right\}$$

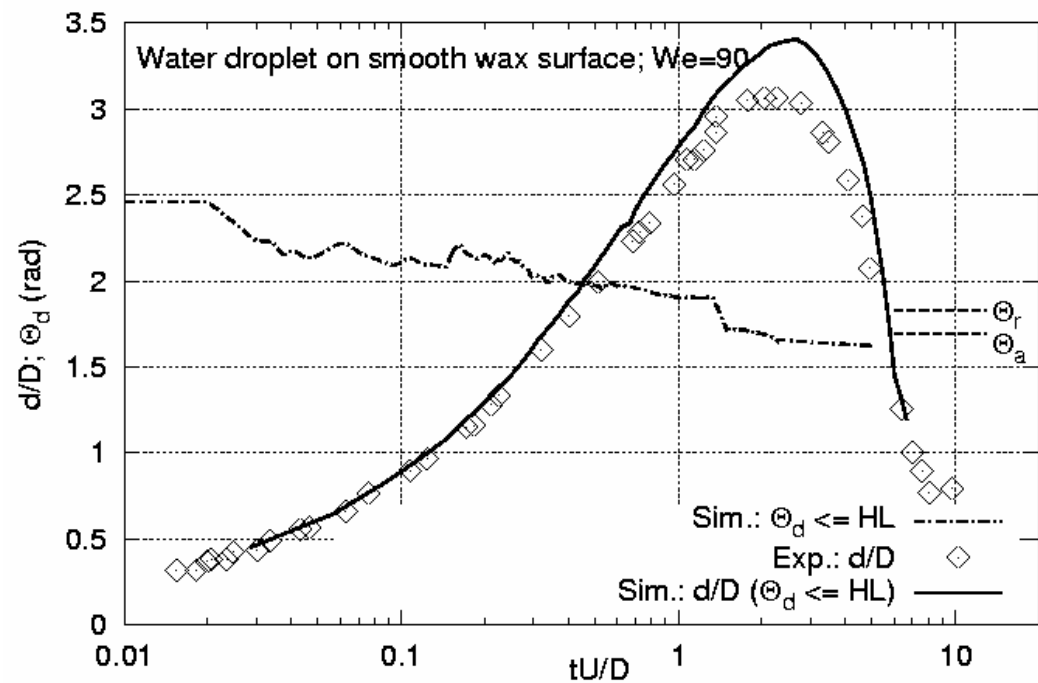
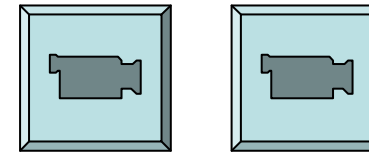
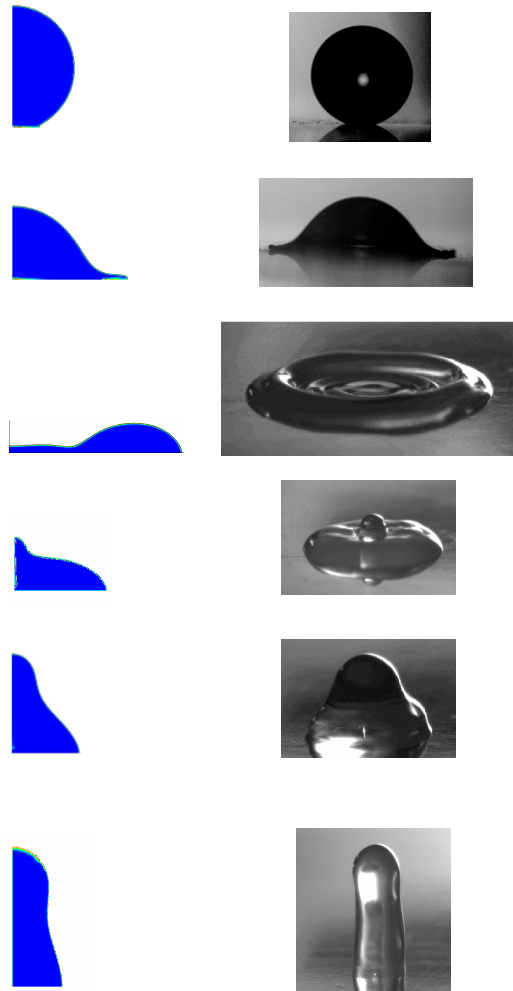
Numerical and experimental drop impact on solid dry surfaces - high wettable surface -



Glycerin droplet on smooth wax/glass surface ($We=90$ - 800): comparison between simulations (left) and experiments (right) at selected time instants

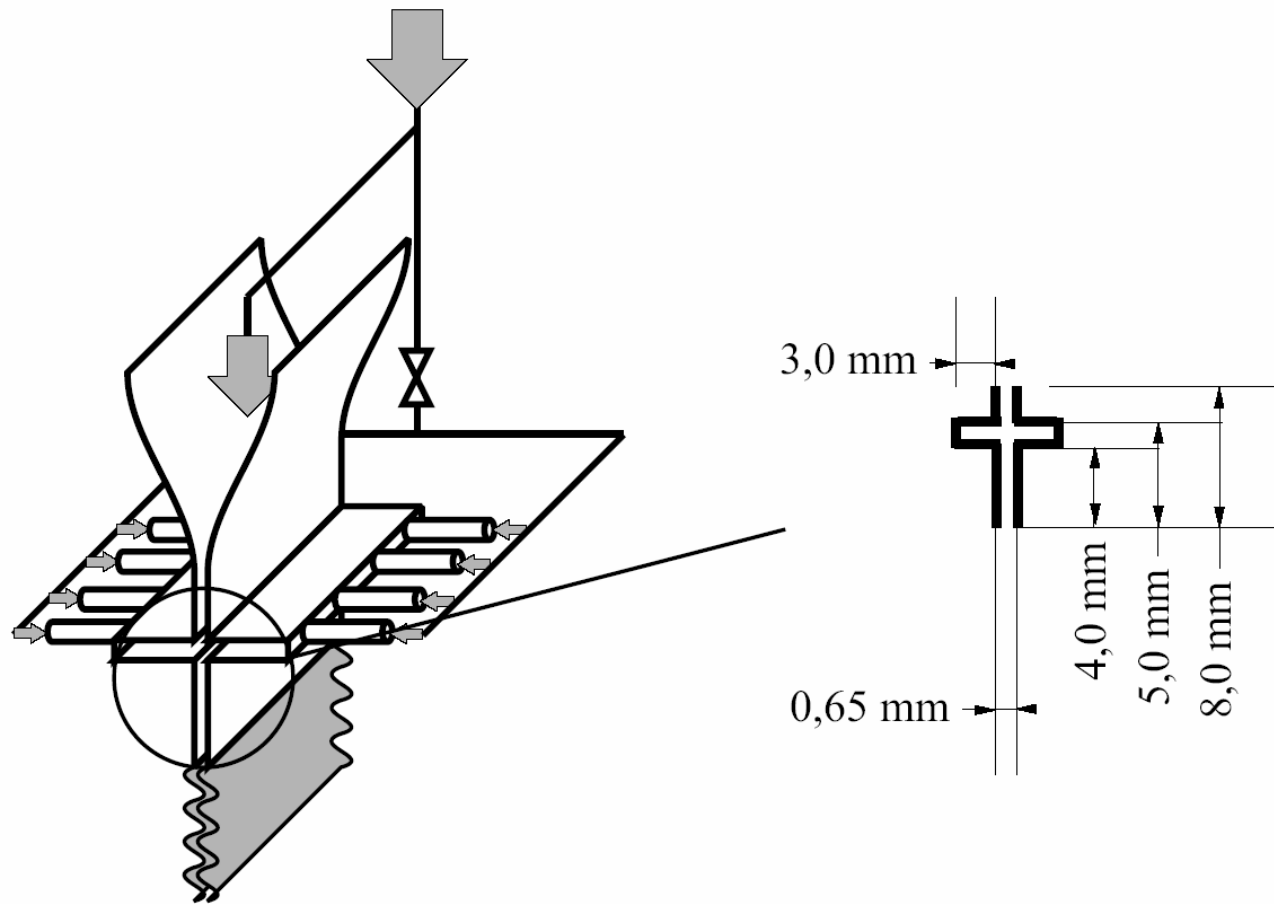


Numerical and experimental drop impact on solid dry surfaces - low wettable surface -

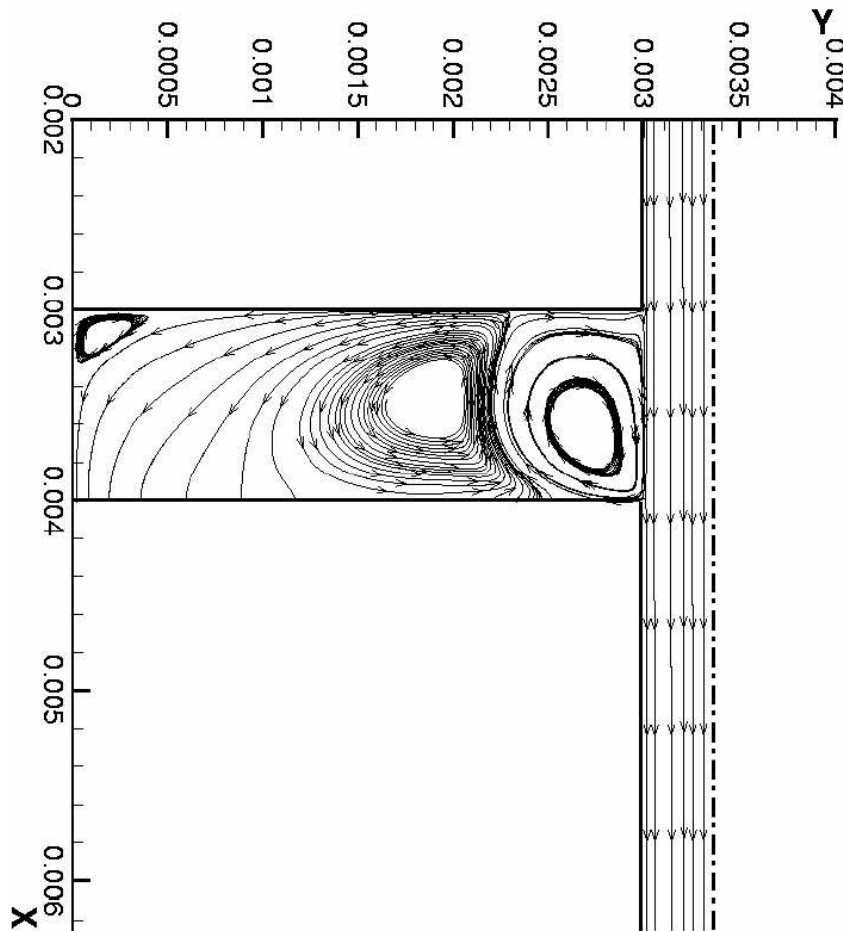


Water droplet on smooth wax surface, $We=90$:
comparison between simulations (left) and experiments
(right) at selected time instants

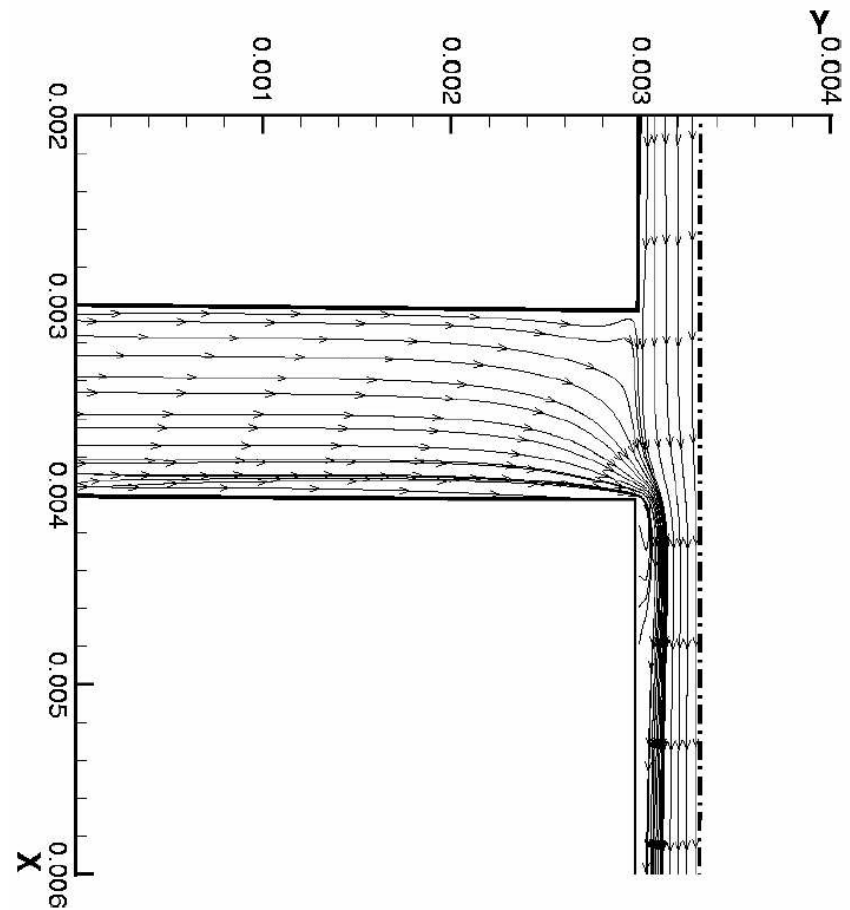
Influence of the inner flow field (turbulence) of flat fan pressure atomizers on the stability of liquid sheets, 1



Influence of the inner flow field (turbulence) of flat fan pressure atomizers on the stability of liquid sheets, 2

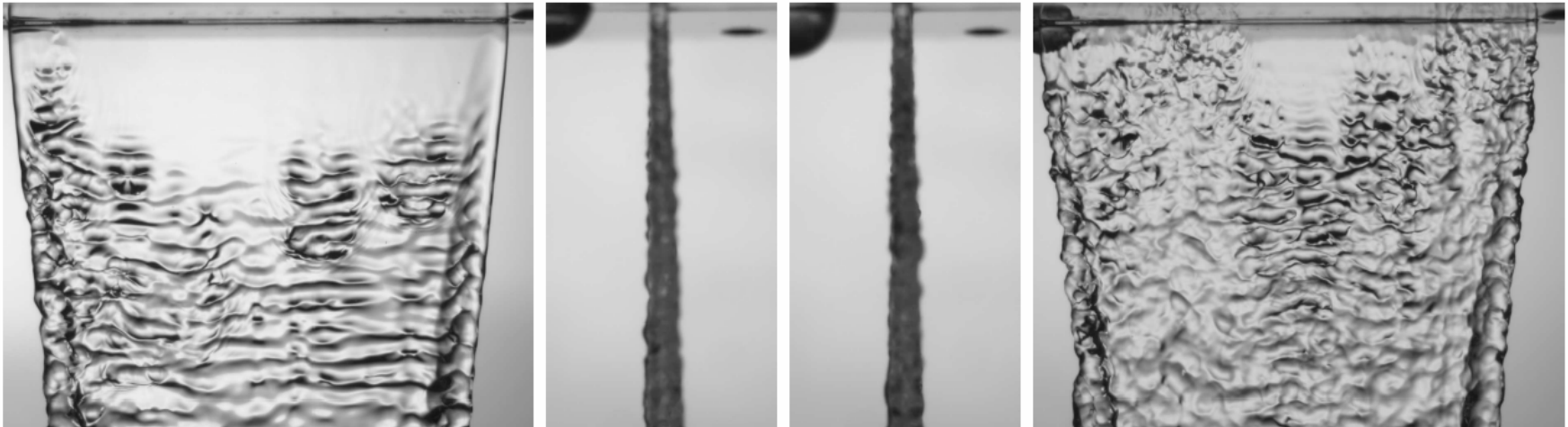


Nozzle B: CLOSED

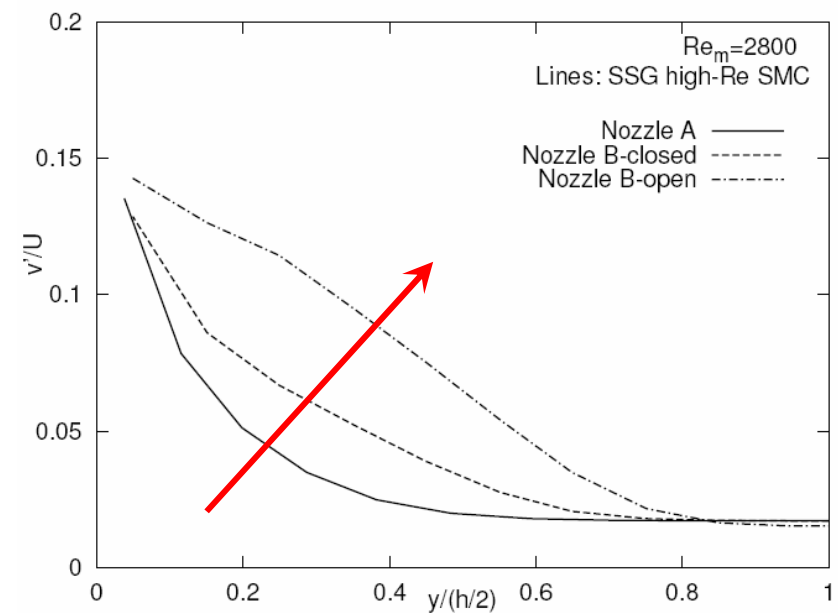
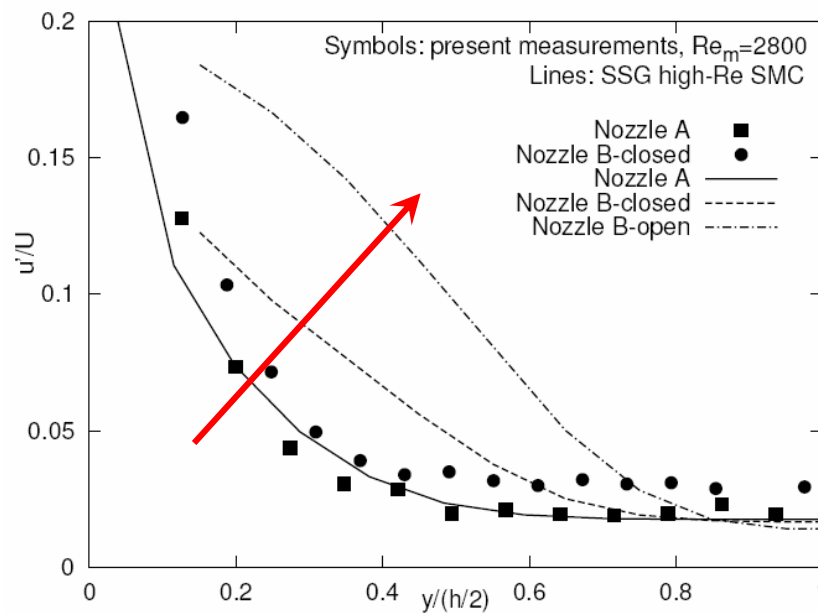


Nozzle B: OPEN

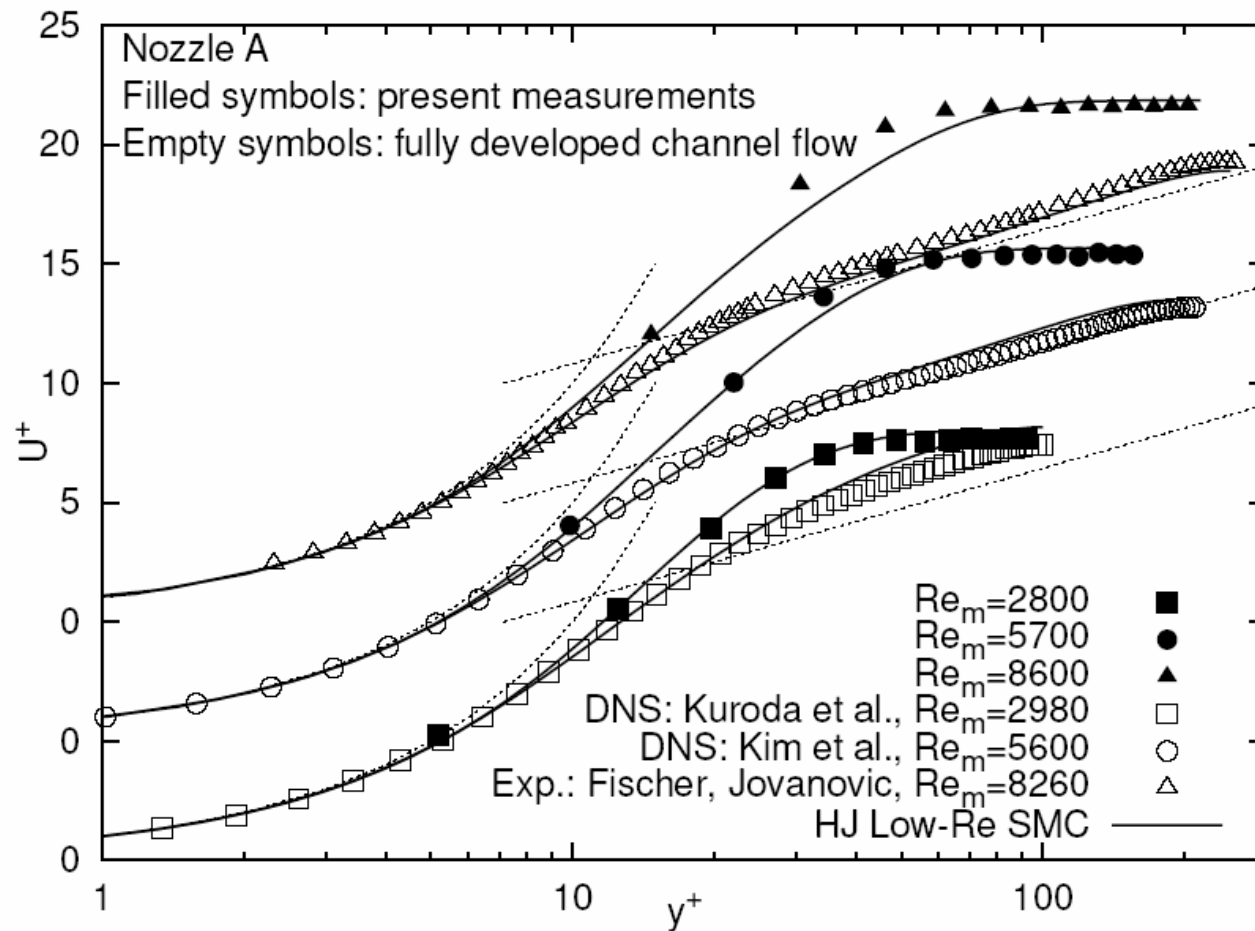
Influence of the inner flow field (turbulence) of flat fan pressure atomizers on the stability of liquid sheets, 3



$Re \approx 3000$; $We \approx 200$ (left: closed tubes; right: open tubes)

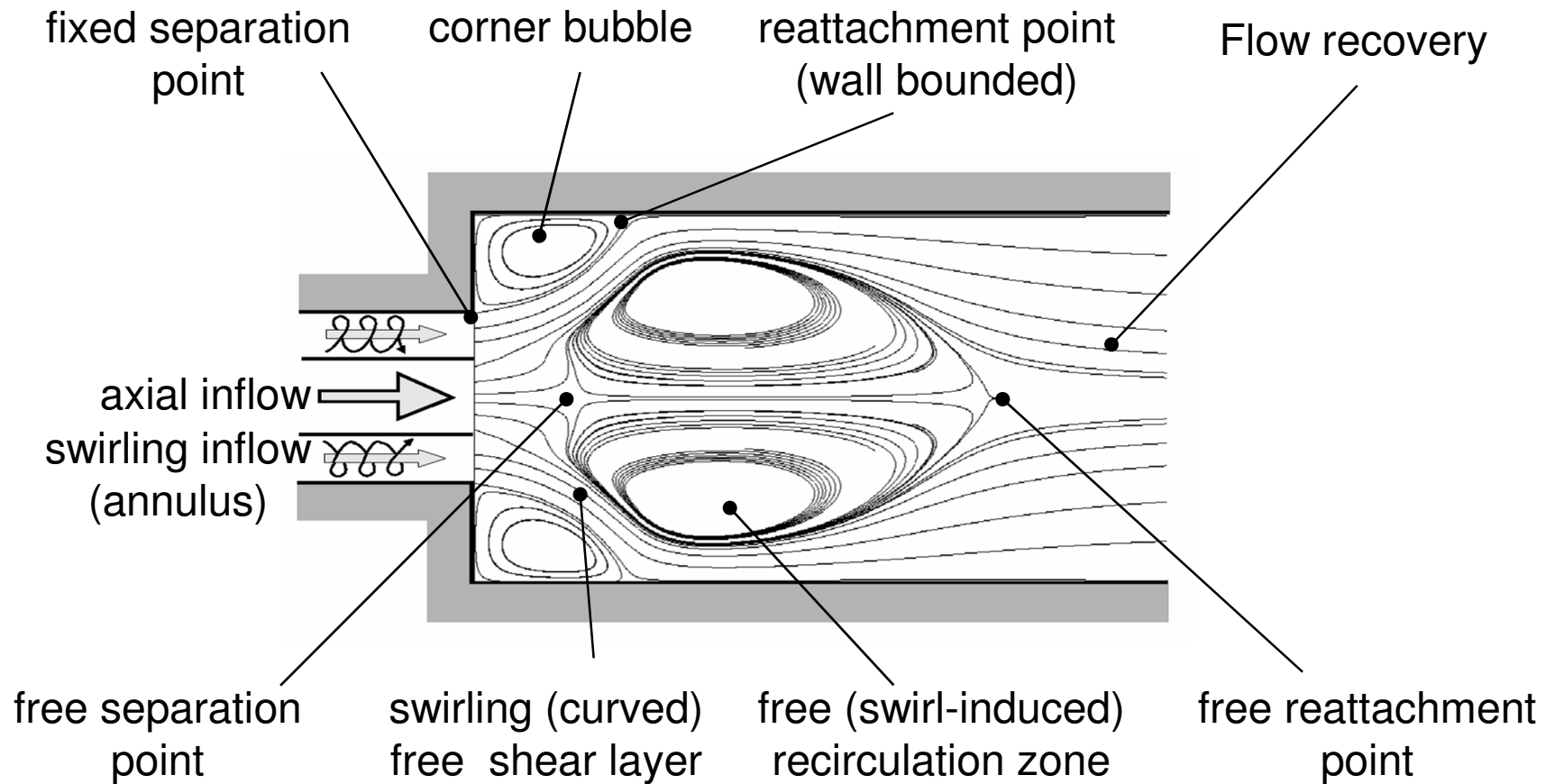


Influence of the inner flow field (turbulence) of flat fan pressure atomizers on the stability of liquid sheets, 4



*Thank you very much for
your attention!*

Isothermal flow in a combustor model: features



- **Complex mean strain tensor: mean and secondary shearing, streamline curvature (local & swirl/transverse), a.p.g. effects, Re-stress anisotropy**

Motivation: Inflow Data Generation

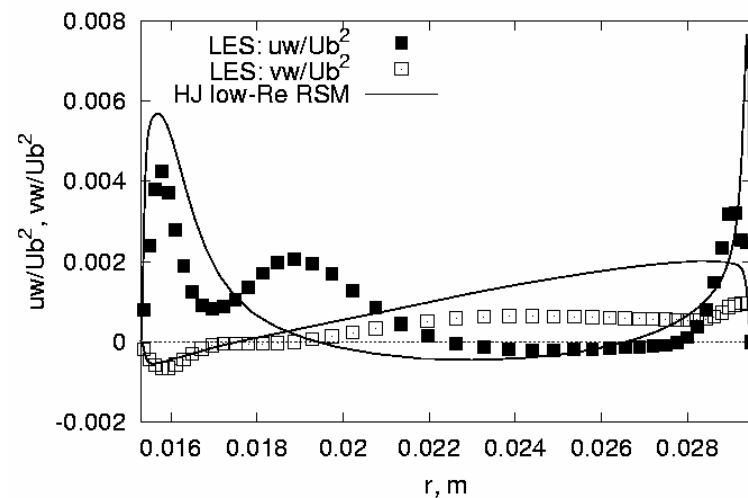
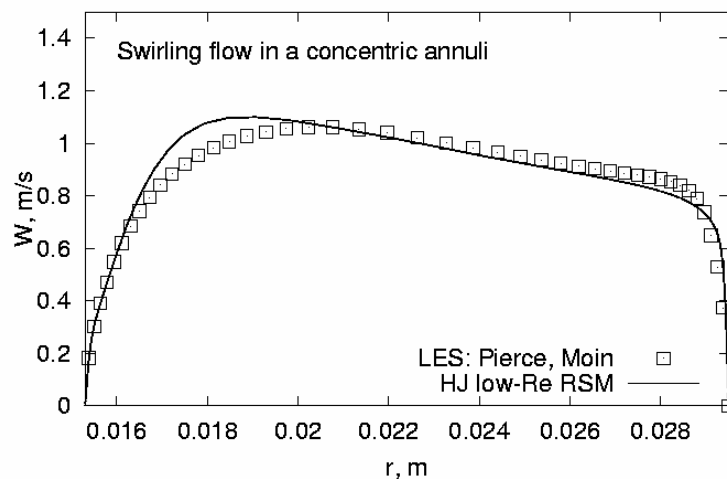
(In line with a LES-based method; Pierce and Moin, 1998)

- Momentum equations for (steady) fully-developed, swirling flow in a pipe

$$\text{U-Vel.: } \frac{1}{r} \mu \frac{\partial^2 r U}{\partial r^2} + \frac{1}{r} \frac{\partial(-\rho r \overline{uv})}{\partial r} + f_x = 0, \quad f_x = -\partial p / \partial x$$

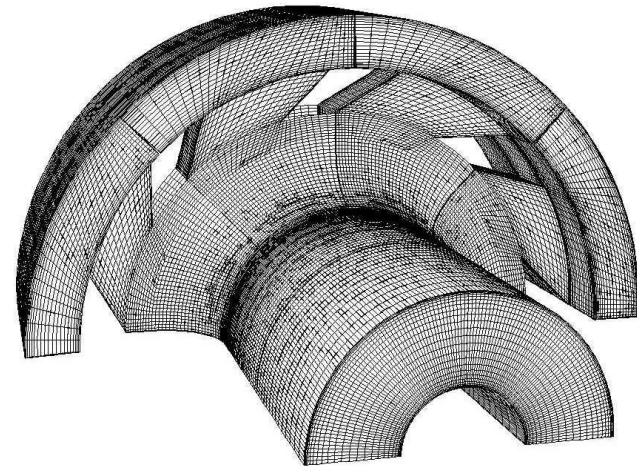
$$\text{W-Vel.: } \frac{1}{r} \mu \frac{\partial^2 r W}{\partial r^2} + \frac{1}{r} \frac{\partial(-\rho r \overline{vw})}{\partial r} - \rho \frac{VW}{r} - \rho \frac{\overline{vw}}{r} + f_\theta = 0$$

- swirl intensity is adjusted by fictitious (constant) body force: $f_\theta \propto \partial p / \partial \varphi$
- low-RSM model used for inflow data generation

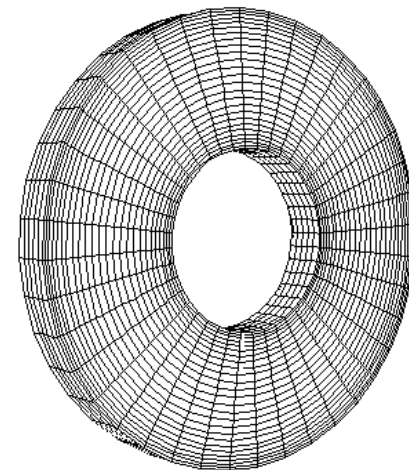


RANS (SMC) computations: swirl generator system and input pipe

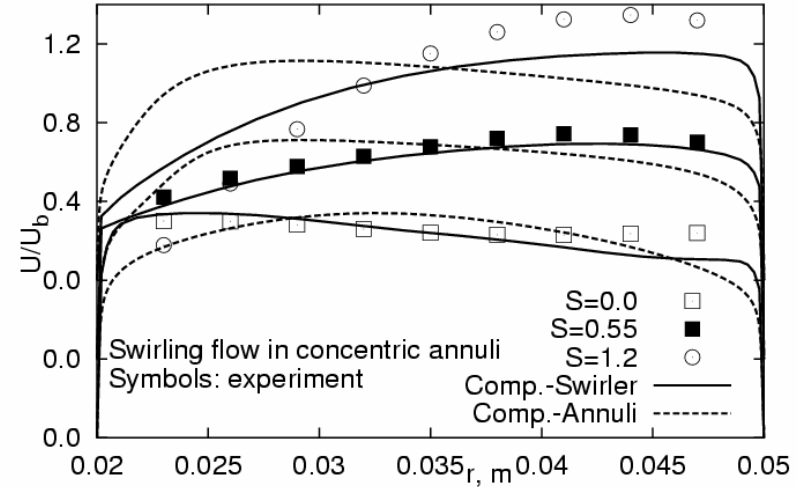
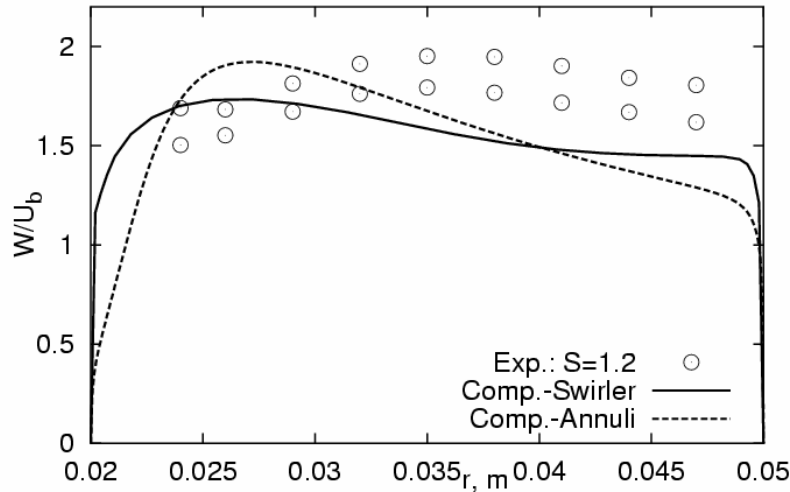
- ➔ 3-D computations (FLUENT) of the inlet section including swirl generator system
 - One eighth of the configuration was accounted for (150.000 cv's)
 - Periodic inlet/outlet in the azimuthal direction; pressure b.c. at the outlet
 - GL RSM (with wall reflection term) + variable model coefficients + enhanced wall treatment (a two-layer treatment based on the 1-eq. k - ϵ model)
- ➔ 3-D computations (FLUENT) of the (fully-developed) swirling flow in a concentric annulus
 - The above-described model was used
- ➔ 2-D (in-house code) of the (fully-developed) swirling flow in a concentric annulus
 - HJ near-wall SMC model (also with eq. for “homogeneous dissipation”)



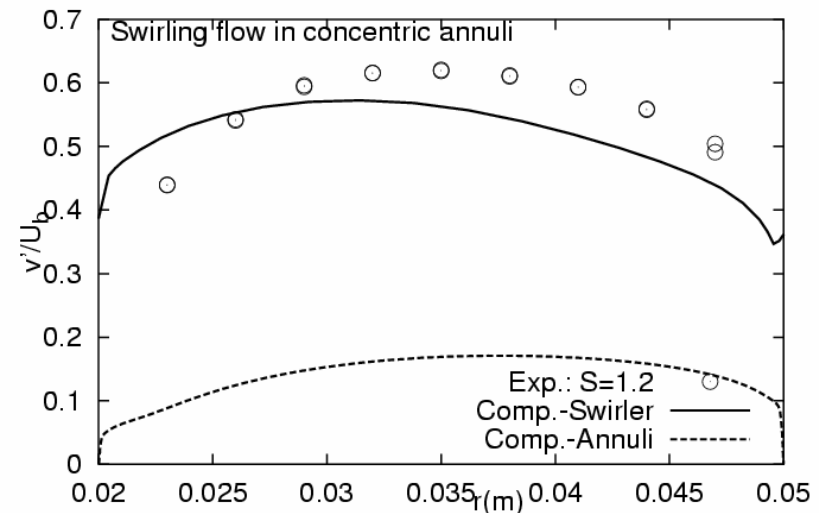
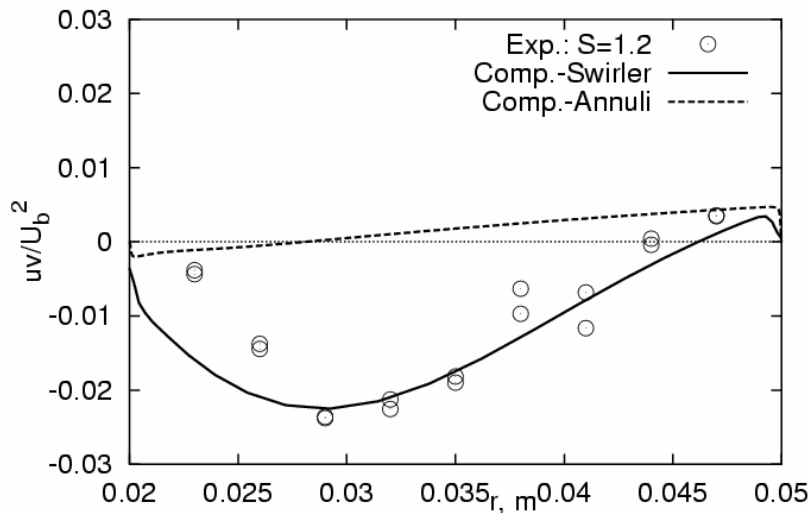
$S=1.2$



RANS (SMC) computations of flow and turbulence in a reality-close swirl combustor: swirl generator and input pipe



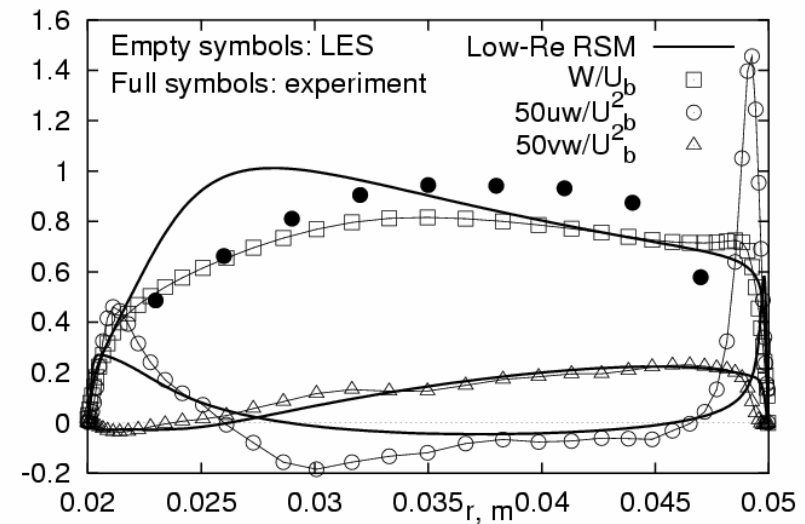
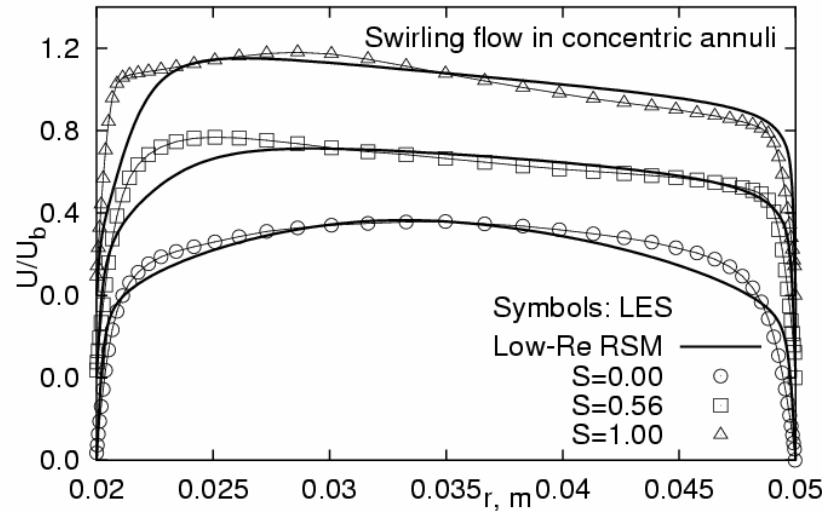
Axial velocity profiles for range of the swirl numbers (left) and circumferential velocity profile for the case with strongest swirl: comparison between experiments and computations



Shear and wall-normal stresses in the concentric annulus of the inlet section of the present model combustor for the case with strongest swirl

RANS (SMC) and LES computations of flow and turbulence in a reality-close swirl combustor: input pipe

Axial velocity profiles for range of the swirl numbers: comparison between LES and RANS computations



Circumferential velocity and corresponding shear stresses in the concentric annulus of the inlet section of the present model combustor for the case with strongest swirl: comparison between LES and RANS computations